HYDRODYNAMICS OF VORTEX SUPPRESSION IN THE REACTOR BUILDING SUMP DECAY HEAT REMOVAL SYSTEM THREE MILE ISLAND NUCLEAR STATION UNIT 2

BURNS AND ROE, INC.

GENERAL PUBLIC UTILITIES

50-320

ALDEN RESEARCH LABORATORIES

February, 1977

HYDRODYNAMICS OF VORTEX SUPPRESSION
in the
REACTOR BUILDING SUMP
DECAY HEAT REMOVAL SYSTEM

THREE MILE ISLAND NUCLEAR STATION
UNIT 2

BURNS AND ROE, INC.

GENERAL PUBLIC UTILITIES

William W. Durgin
Lawrence C. Neale
Richard L. Churchill

George E. Hecker, Director

ALDEN RESEARCH LABORATORIES
WORCESTER POLYTECHNIC INSTITUTE
HOLDEN, MASSACHUSETTS 01520

February, 1977

TABLE OF CONTENTS

ACKNOWLEDGEMENTS

Not long after a final report on a research project is completed, the conditions prevailing at the time are quickly forgotten. In this case, the concluding experiments and this report on the findings were performed and prepared under a greatly shortened schedule, and we would like to take this opportunity to express our gratitude to those responsible for meeting that schedule.

Thanks to Wayne Parmenter, Bryan Hmura and James Ushiburnis, for their work on the drawings and photographs. Nancy Vacca, for her patience in typing and retyping the text, and Diane Gramer and Richard Van Leeuwen for their help in editing and final testing.

ABSTRACT

General Public Utilities contracted Burns and Roe, Inc. to design the Three Mile Island Nuclear Station, Unit No. 2, located on the Susquehanna River near Middletown, Pennsylvania. To establish the outflow characteristics of the reactor sump for the decay heat removal system, the Alden Research Laboratories was authorized to construct and test a hydraulic model of the reactor sump and surrounding area.

The main purpose of the study was to verify that the reactor sump would properly drain the emergency cooling water without the development of free surface vortices or other flow irregularities which might adversely influence the operation of the decay heat removal system. In the event that undesirable flow conditions occurred, means of improving flow patterns were to be developed.

Tests of the 1:3 scale model showed that the original design could be improved with respect to free surface vortices. Considering the prototype operating conditions and possible scale effects on modeling vortices, it seemed desirable to improve the flow characteristics. Various changes to the screens were made, and grids were installed over the sump to attenuate flow rotation. Tests at increased model flow rate and water temperatures were conducted to investigate possible scale effects on vortices, and the resulting data indicated that the recommended prototype installation will operate satisfactorily.

INTRODUCTION

Burns and Roe, Inc. was contracted by General Public Utilities to design the Three Mile Island Nuclear Station, Unit No. 2. As usual, the plant is provided with an emergency flow system to cool the shut-down reactor in the unlikely event of a loss of coolant accident. Water from the reactor coolant system, and from emergency core cooling system storage tanks, will be released within the containment building, ultimately draining to the reactor building decay removal sump. When the external supplies of water are depleted, the suction of the decay heat removal and reactor building spray pumps will be automatically transferred from the storage tanks to the decay heat removal sump, to provide a continuous supply of water for emergency core cooling and the building spray header in the reactor containment building dome. For proper operation of the decay heat removal system, the sump geometry must induce flow patterns which are free of air drawing vortices and minimize energy losses, particularly at the pipe entrances.

Alden Research Laboratories (ARL) was commissioned to construct and test a model of a portion of the reactor containment building and the entire sump to determine flow characteristics. Potential problem areas investigated were free surface vortex formation, other undesirable flow patterns, and energy losses. Various means of improving the flow characteristics were investigated. Special attention was given to potential scale effects of free surface vortices by operating the model at elevated temperatures and higher than scaled flow rates.

This report presents a description of the prototype and model, and summarizes model construction, instrumentation, and test procedures. Appropriate test results and a recommended final design are included.

PROTOTYPE DESCRIPTION

The reactor building sump is part of the decay heat removal system. The sump is located in a compartment between the secondary shield wall and the containment wall, as shown in Figure 1. The sump is basically a rectangular pit in the reactor building floor about 6 ft deep. Two 18 inch lines, Figure 2, connect the sump to

the decay heat removal system pumps, which provide flow to heat exchangers and a spray system. Various floor gratings and screens are proposed to prevent debris from entering the two lines.

The sump floor is at elevation 276.5 ft and the reactor building floor is at elevation 282.5 ft. The water level in the reactor building resulting from a loss of coolant accident (LOCA) will be between elevation 286.0 ft and 289.0 ft. The total flow to the sump area will not exceed 12,000 gpm, and approach the sump either fully from the east wing of the reactor building, fully from the west wing, or from both sides of the building in any proportion. Each of the two 18 inch diameter sump outlet pipes is designed for a maximum capacity of approximately 6,000 gpm, and one or both outlet pipes may be in operation at any given time.

During the recirculation mode of emergency operation, the pressure and temperature in the reactor building would range from atmospheric to 7 psi gauge, and 60F to 230F, respectively. The indicated range of pressures will not affect the flow patterns. However, the changes in water density and viscosity resulting from the temperature variation were considered in designing the model and in developing the test program.

SIMILITUDE

To properly simulate the kinematics and dynamics of the fluid flow field, an undistorted geometric model was required. In addition, gravitational and inertial forces dominated the flow processes involved, so that basic similarity of the fluid mechanics was achieved through Froude scaling. The Froude number, representing the ratio of inertia to gravitational force,

$$F = u/\sqrt{gs} \qquad (1)$$

where

u = average pipe velocity

g = gravitational acceleration

s = submergence

was made equal in model as in prototype

$$\mathbb{F}_r = \frac{\mathbb{F}_m}{\mathbb{F}_p} = 1 \qquad (2)$$

where m, p, r, are model, prototype, and ratio between model and prototype, respectively. Velocity, flow rate, and time, u, Q, t, respectively, can be expressed in terms of the chosen geometric scale

$$l_r = \frac{l_m}{l_p} = 1/3$$

where l refers to length. By use of Equations 1 and 2 with $g_r = 1$,

$$u_r = l_r^{1/2} = 1/1.73$$

$$Q_r = l_r^{5/2} = 1/15.6$$

$$t_r = l_r^{1/2} = 1/1.73$$

The flow field also depends on viscous and possibly surface tension effects. The relative magnitudes of these forces to fluid inertia are reflected in the dimensionless groups called Reynolds number and Weber number, respectively:

$$\mathbb{R} = u\,d/\nu \qquad (3)$$

$$\mathbb{W} = \rho\,u^2 s/\sigma \qquad (4)$$

where

d = pipe diameter
ν = kinematic viscosity
ρ = density
σ = surface tension
s = submergence

For models under Froude scaling, these groups generally cannot have the same values as they do in the prototype. Any deviation in similitude of the flows attributable to viscous and surface tension forces was called scale effect. Surface tension effects only became important when there was strong surface curvature. In a situation where a strong vortex was unacceptable, the free surface was essentially flat, and surface tension scale effects were not important. Vortex severity, S, was, therefore, predominantly a function of Froude number, possibly with some Reynolds number scale effect

$$S = S(\mathbb{F}, \mathbb{R}) \tag{5}$$

If the reduction in model Reynolds number compared to the prototype could result in significant scale effects, some type of prediction technique was necessary (1). Free vortices can be classified according to visually differentiable types, and Figure 3 shows a reasonable delineation from a swirl, Type 1, to a continuous air entraining vortex, Type 6. It was necessary to establish how a particular vortex strength in the model can be transferred to the prototype.

Figure 4 illustrates a proper method of projecting model results to the prototype. The ordinate was the ratio of model to prototype Froude number, and this parameter would be unity for model operation under Froude scaling, while the abscissa was the Reynolds number. Assuming that the model was operating at Froude scaling at point a_1, the effect of increasing the discharge in the model (at constant temperature) was to increase both $\mathbb{F}_r$ and $\mathbb{R}$, to point a_2. Assuming that the formation of some vortex strength, Type N, was of interest, the discharge should be increased until that vortex was observed, say at point a_4. The model Reynolds number can also be changed by varying the kinematic viscosity, as with temperature, and similar tests performed to locate b_3, another point on the locus of Type N vortices. Extrapolation of the line of constant vortex strength can be made to a prototype Reynolds number at the proper Froude number ($\mathbb{F}_r = 1$), point p_1. For large prototype $\mathbb{R}$, point p_2, greater asymptotic behavior will be expected, in keeping with trends of other fluid mechanic phenomena.

The locus could also be of any other expedient measure of vortex severity. The inlet loss coefficient (alternatively the coefficient of discharge) was shown to be dependent on circulation (2) and may form a measure of vortex severity. Additionally, angular momentum of the flow was approximately conserved through the inlet since tangential shear was small (3). The angle of indicated swirl was $\alpha = \tan^{-1} \pi n d/u$ (4), where n equals angular velocity as measured by a crossed vane vortimeter. Provided the velocity profiles in the pipe were reasonable, that is, there was not a concentrated vortex core in the region of the meter, the vortimeter angular velocity was a measure of angular momentum of the flow, and hence of vortex severity (5). Thus, in addition to visual observations as the primary classification of vortex type, both loss coefficients and vortimeter angular velocity can reflect vortex severity.

Model velocities were increased up to 70% above Froude scaled values to aid projection to prototype operation. Additionally, both model and prototype could operate at elevated temperatures, giving rise to a Reynolds number range in each case.

TABLE I

Range of Prototype and Model $\mathbb{R}$

Prototype

	6,000 gpm Each Line
T = 60°F	$\mathbb{R} = 1.1 \times 10^6$
T = 230°F	$\mathbb{R} = 3.9 \times 10^6$

Model

	$\mathbb{F}_r = 1$	$\mathbb{F}_r = 1.5$	$\mathbb{F}_r = 1.7$
T = 60°F	$\mathbb{R} = 2.0 \times 10^5$	$\mathbb{R} = 3.0 \times 10^5$	$\mathbb{R} = 3.4 \times 10^5$
T = 160°F	$\mathbb{R} = 5.1 \times 10^5$	$\mathbb{R} = 7.6 \times 10^5$	$\mathbb{R} = 8.7 \times 10^5$

For an intake head loss, h_l, the loss coefficient

$$K = \frac{h_l}{u^2/2g}$$

was an Euler number dependent on the other non-dimensional groups, that is

$$K = K(\mathbb{F}, \mathbb{R}).$$

The sump and intake head loss was computed by subtracting the velocity head from the static head change, Δh, between the free water surface and the pipeline pressure gradient extrapolated to the inlet.

$$h_l = \Delta h - u^2/2g$$

MODEL DESCRIPTION AND INSTRUMENTATION

A physical model, Figure 5, of the reactor building sump, and a portion of the sump approach area, was constructed to a uniform scale of approximately 1:3 on an elevated platform. A portion of the outlet piping was also modeled. The overall size of the model was approximately 41 ft long, 15 ft wide, and 5 ft high, and it was located in one of ARL's buildings.

The reactor building portion of the model was constructed of 1/4 inch steel, and painted with a rust inhibiting paint. The sump walls and floor, shown in Photograph 1, were constructed of 1/2 inch thick plexiglass in a steel frame to allow observation of the flow patterns and provide access for necessary data collection and documentation through photography. Clear acrylic outflow pipes were installed for visual observation of flow patterns.

In modeling the reactor building sump room, all piping, pumps, motors, and electrical devices were scaled and installed, as shown in Photograph 2. The area approaching the sump room also included the scaling and installation of cabinets, pumps, support columns, tanks, and miscellaneous equipment that could have an influence on the flow patterns, Photographs 3, 4, 5, and 6.

A vortimeter was used for detecting and counting swirl conditions in the outflow pipes, Photograph 7. The vortimeter was installed in outflow line 1, as shown in Figure 6.

ASME standard orifice meters were used to determine flow rates in each outlet pipe, and measurement of the differential pressure across the orifice plate established flow rates. The head needed to achieve the gravity driven flow was provided by constructing the model on an elevated platform. Flow was supplied to the model by a 24 inch line from a vertical pump, and the supply line entered the floor of the model behind the simulated secondary shield wall. An adjustable overflow weir was provided to balance the inflow and outflow and regulate water depth.

Preliminary data for head loss were recorded at one and four diameters on both outflow pipes. For the final configuration, pressure measurements were taken at each diameter along the outfall line 2 so that the hydraulic gradeline could be well established. The pressure tap arrangement is shown in Figure 6 and Photograph 8. Pressures were read with a manometer to 0.001 ft.

The elevated temperatures were obtained by using a 50 HP boiler to heat water in the reservoir of the building. Two inch thick sheets of styrofoam insulation were floated on the water surface of the building reservoir to prevent heat loss. The model, with the exception of the reactor building sump room, was also enclosed with polyethylene sheeting. A dial thermometer was installed in each of the outflow lines downstream of the orifice meter for observing the water temperature during a test. The system was capable of maintaining a water temperature of approximately 150-170°F.

TEST PROCEDURE AND CONDITIONS

Tests were conducted in two phases. Phase 1 tests consisted of setting up and observing many selected modifications utilizing baffles, flow straighteners, and screen designs. Phase 2 tests consisted of a detailed study of the proposed final design, particularly for potential scale effects related to free surface vortices.

A test was initiated by filling the model with water and purging air from the outlet pipes and manometer lines. The manometer was checked for zero deflection at zero flow. Water temperatures were then measured and recorded, and the manometer deflection corresponding to the desired flow rate was set for the given temperature conditions. The water level in the model was adjusted by the overflow weir in the reactor containment portion of the model. At least fifteen minutes was allowed for the flow in the model to reach steady state conditions.

Overall flow patterns were recorded photographically using tufts of yarn on a grid parallel to the floor of the sump at an elevation of 280.1 ft. The two inch tufts of yarn were mounted at the intersection of a fine wire grid at four inch by four inch spacing, as shown in Photograph 8.

Vortimeter rotations were recorded for all tests of the final design. When flow conditions were considered stable, a fine mesh screen was used to remove all surface debris, and also any debris buildup on the screen for tests of unblocked screens. Three sets of readings with an automatic counter were taken, each reading being preset so that the revolutions per one hundred seconds was obtained. While the revolutions were being counted, the direction of rotation was observed while looking downstream, and recorded as being clockwise or counter-clockwise. Observations were also recorded as to the type of vortex, according to the vortex strength scale of Figure 3.

Photographs were taken of dye injected at pertinent points on the water surface. Pressure readings were read and recorded at taps 1 through 10 diameters downstream of the entrance of the outflow line 2 on all Phase 2 tests.

The model tests were conducted at room temperature for the basic test program and check tests were run at elevated temperatures (140-170°F) during Phase 2. Test conditions simulated maximum design flow per pipe, partial flow per pipe, maximum and minimum water depths in the containment, grating and screen blockage, and the direction of approach flow to the reactor building sump.

Appendix A lists the tests and operating conditions, while Figures 7 to 10 illustrate the basic schemes examined.

Early in the program, many suggested schemes were evaluated. These are called Schemes 1-11 and comprise Phase 1 of the test program. Scheme 12, the final design configuration, was used exclusively in Phase 2 testing, with the exception of the removal of the gratings (vortex suppressors) during some comparison tests.

RESULTS AND DISCUSSION

Scheme Development

Figures 7 through 10 show the various schemes which were tested to minimize swirl and potential vortex activity in the sump. In developing the schemes, visual free surface observations, the string grid, and dye injection were used as indicators of vortex activity and flow patterns.

Scheme 1, shown on Figure 6, had 1 inch by 4 inch engine grating at the east and west access doors, and an elevated platform that provided access to an overhead valve. The platform legs shed vortices of sufficient intensity to reject this arrangement.

Scheme 2, Figure 7, had only the engine grating at the east and west access doors. The shedding of vortices from the piping of the waste section of the sump was sufficient to discourage further testing.

Scheme 3 had the 1 inch by 4 inch engine grating at the east and west access doors with a divider wall, as shown in Figure 7. Vortex shedding from the piping of the waste section of the sump remained objectionable.

Scheme 4, Figure 7, was the same as Scheme 2 except for the addition of a 15 inch H beam as a flow deflector. This beam was installed in an attempt to prevent the shedding of the vortices from the piping. The arrangement did not attenuate swirl to acceptable limits.

Scheme 5, Figure 8, had the 1 inch by 4 inch engine gratings at the access doors and a screen with frame encompassing the entire sump. This reduced the effect of vortex shedding from the piping, but not sufficiently to alleviate all concerns.

Scheme 6, Figure 8, incorporated the same screen and engine grating arrangement as Scheme 5, with the addition of a 45° inclined baffle, with the bottom at elevation 284.0 ft. This arrangement was effective for a particular water depth, but could not eliminate vortex activity at all water depths.

Scheme 7, Figure 8, utilized the same screen and engine grating arrangement as Scheme 5, with a horizontal baffle at elevation 285.5 ft. Similar depth sensitivity results as with Scheme 6 were found.

Scheme 8, Figure 9, had the engine grating at both east and west access doors, with a screen and frame system 7.0 ft high, and covering only the 4.5 ft by 7.5 ft rectangular decay heat removal section of the sump. The 7.5 ft section of screen was at an angle of 10° with the vertical to avoid interference with valves in the waste removal section of the sump. Vortices were shed from the corner post of the screen support system.

Scheme 9, Figure 9, had the same engine grating and sump screen design as Scheme 5, with the addition of a vortex suppressor grating at elevation 285.5 ft. The grating had a 4.5 inch by 4.5 inch square grid, and a 6.0 inch depth. This scheme produced good performance and minimized vortices.

Scheme 10, Figure 9, had the engine gratings at the east and west access doors, with a sump screen 4.5 ft by 11.5 ft by 6.75 ft in height and using 1/4 inch centerline #10 wire screen mesh. This scheme had satisfactory results in minimizing vortex activity.

Scheme 11, Figure 9, had the same engine grating and sump screen as Scheme 10. In addition, the vortex suppressor grating design of Scheme 9 was installed at elevation 285.5 ft. This scheme eliminated vortex activity in the area of concern under normal operating conditions. However, when the east access door was totally blocked, the free water surface in the sump room dropped below the elevation of the vortex suppressor, eliminating its attenuating effect on swirl.

Scheme 12, Figure 10, utilized a large cage of engine grating at the east doorway, Photographs 10 and 11, in order to increase the surface area for maintaining sufficient flow in case of blockage by debris. An additional vortex suppressor was installed at elevation 282.5 ft to eliminate any potential for vortex formation at low water levels, which could be caused by nearly total blockage of the east doorway. Flow patterns in the sump, as indicated by the string grid, were favorable inasmuch as no areas of separation or reverse flow were observed.

The two horizontal vortex suppressors at elevation 285.5 ft and 282.5 ft were designed as square grids with 0.375 ft by 0.375 ft openings and a depth of 0.5 ft in an "egg crate" arrangement. The dimensions of the upper grating were 10.75 ft by 3.94 ft and the lower was 7.0 ft by 3.75 ft. The gratings were enclosed within the rectangular sump screening, which consisted of two panels 11.5 ft and 4.5 ft each 6.75 ft high. The screen support frame scaled 4 inch by 4 inch steel angles, bolted to the sump room floors and walls, Figure 11. The screen, with 1/4 inch centerline #10 wire mesh, was mounted on the frame shown in Photograph 12. The west access door had 1 inch by 4 inch engine grating as a trash rack for stopping debris from entering the sump room, as shown in Photograph 5, while the east access door also had engine grating, as shown in Photograph 3.

Loss Coefficients

Figure 12 shows the variation of entrance loss coefficients for both sump withdrawal lines with Reynolds number, for the indicated schemes. K_1 is the loss coefficient for the south line, and K_2 represents the north line. For each scheme, the values of K_1 were higher than K_2 by about 25% at corresponding Reynolds numbers. It

was noted that the intake for line 1 was more confined geometrically than line 2 and that generally greater vortex activity was present than at line 2. The data scatter are due to the preliminary pressure readings, as compared to the subsequent refined piezometric gradeline extrapolation to the intake of the final scheme. The trend with Reynolds number was similar for each coefficient with values of K_1 and K_2 increasing with increasing Reynolds number and showing a tendency to level off at approximately $\mathbb{R} = 10^6$.

For the final design, Scheme 12, loss coefficients were only obtained for line 2 because the vortimeter was installed in line 1. A continuous length of plastic pipe was used to establish the pressure gradeline and values of K_2 were from tests taken at temperatures ranging from 60°F to 170°F. Figure 13 shows that as the Reynolds number increased, values of K_2 also increased.

The trend of loss coefficient with $\mathbb{R}$ was unusual in that intake loss coefficients usually decrease with increasing Reynolds number. With swirl present, however, the coefficient can increase with increasing Reynolds number (2).

Tests of Proposed Design, Scheme 12

A comprehensive series of tests was run for the proposed final design, Scheme 12, and the test conditions are summarized in Table II. The basic variables were water elevation, flow, and temperature, and the Froude and Reynolds numbers were thus varied over limited ranges. The vortex type and vortimeter rotation were the experimentally measured quantities. In addition to the main test series, for which the suppressors were in place, both lines were running, and the flow assumed its natural division between the approach paths, tests were also conducted without the vortex suppressors in place, with the discharge lines running individually, and with flow approaching the sump room with the doorways alternately blocked.

TABLE II
TEST RESULTS - SCHEME 12

LEVEL FT	FLOW GPM	TEMPERATURE °F	VORTEX SUPPRESSOR	F_r	$R \times 10^{-5}$	VORTEX TYPE	ANGULAR VELOCITY	TEST NO.	
286	6,000	65	N	1.0	1.9	2	0.46	02-007	
286	6,000	60	N	1.0	1.9	1,2	0.48	02-003	
286	6,000	159	N	1.0	5.2	4	0.44	02-021	
286	9,000	60	N	1.5	2.8	$Q_1 = 4,5$ - $Q_2 = 2$	0.40	02-028	
286	6,000	50	Y	1.0	1.6	0	0.20	02-004	
286	6,000	60	Y	1.0	1.9	0	0.12	12-01	
286	6,000	60	Y	1.0	1.9	0	0.20	02-005	
286	6,000	80	Y	1.0	2.4	0	0.18	02-010	
286	6,000	90	Y	1.0	2.7	1	0.16	02-011	
286	6,000	100	Y	1.0	3.0	1	0.15	02-012	
286	6,000	100	Y	1.0	3.1	1	0.18*	01-07	
286	6,000	110	Y	1.0	3.4	1	0.20	02-013	
286	6,000	120	Y	1.0	3.8	1	0.18	02-014	
286	6,000	130	Y	1.0	4.0	*	0.22	02-015	
286	6,000	140	Y	1.0	4.4	1,2	0.28	01-08	
286	6,000	140	Y	1.0	4.4	1	0.24	02-016	
286	6,000	150	Y	1.0	4.6	1	0.15	02-017	
286	6,000	170	Y	1.0	5.5	1,2	0.14	01-09	
286	6,000	170	Y	1.0	5.5	1,2	0.10*	01-09	
286	6,000	60	Y	1.0	1.9	TURBULENT	0.30	02-001	Q_N ONL
286	9,000	60	Y	1.5	2.8	1	0.30*	02-022	
286	9,000	172	Y	1.5	8.2	1,2	0.11	01-10	
286	6,000	60	Y	1.0	1.9	0	0.08*	12-02	Q_E ONLY
286	6,000	60	Y	1.0	1.9	1	0.25*	01-01	Q_1 ONLY
286	6,000	60	Y	1.0	1.9	0	0.00	01-02	Q_2 ONLY
286	6,000	70	INDUCED VORTEX	1.0	2.1	6	0.40	02-009	
286	2,500	60	Y	0.4	0.8	0	0.03	01-03	
286	2,500	62	Y	0.4	0.8	0	0.10*	01-04	Q_1 ONLY
286	2,500	62	Y	0.4	0.8	0	0.00	01-05	Q_2 ONLY
286	6,000	62	Y	1.0	1.9	0	0.5	01-06**	
289	6,000	60	N	1.0	1.9	2	0.46	12-027	
289	9,000	60	N	1.5	2.8	$Q_1 = 4,5$ - $Q_2 = 3,4$	0.67	02-025	
289	9,000	155	N	1.5	7.1	3,4	0.62	02-020	
289	10,400	60	N	1.7	3.4	$Q_1 = 4,5$ - $Q_2 = 3,4$	0.68	02-026	
289	10,400	155	N	1.7	8.2	4,5	0.59	02-019	
289	6,000	60	Y	1.0	1.9	1	0.22	02-002	
289	6,000	166	Y	1.0	5.1	1	0.27	01-12	
289	9,000	60	Y	1.5	2.8	2	0.16	02-024	
289	9,000	165	Y	1.5	7.6	1,2	0.27	01-11	
289	10,400	155	Y	1.7	8.2	1	0.39	02-018	
289	10,400	60	Y	1.7	3.4	1,2	0.22	02-023	

*CCW ROTATION
**UPPER 50% OF SUMP SCREEN BLOCKED

57-217

ARL

Figure 14 shows the vortimeter angular velocity and observed vortex type versus Reynolds number, with the water surface at elevation 286 ft and at a Froude number ratio of one (i.e., the prototype Froude number). With the vortex suppressors in place, the angular velocity was always between 0.10 and 0.30 sec^{-1} and showed no tendency to increase with Reynolds number in the range of 1.6×10^5 to 5.5×10^5. Without the suppressors, the angular velocity was between 0.4 and 0.5 sec^{-1}. A Type 6 vortex was intentionally induced using two boards, with the suppressors removed, also producing an angular velocity of 0.4 sec^{-1}. This indicated that the angular velocity of the vortimeter was not a sensitive indicator of strong vortices with small coherent cores. Furthermore, due to the weak relation between vortex type and angular velocity, particularly with the vortex suppressors in place, primary emphasis was placed on the vortex strength observations.

The vortex strength increased with Reynolds number, with and without suppressors. With suppressors, the severity increased from Type 0 to Type 1 and 2 for $1.6 \times 10^5 < \mathbb{R} < 5.5 \times 10^5$. To extend these trends to the prototype operating range, it is necessary to refer to changes in swirl intensity with Reynolds number. Figures 12 and 13 showed that the entrance loss coefficient became independent of Reynolds number at about $\mathbb{R} = 10^6$. Since only swirl affects the loss coefficient in this range of $\mathbb{R}$ (2), it may be concluded that swirl intensity would not increase above $\mathbb{R} = 1 \times 10^6$. Therefore, no vortices stronger than Type 3 seem possible in the prototype.

Figures 15 through 18 show the test results in the Froude number ratio versus Reynolds number plane. For each data point, the vortimeter angular velocity (sec^{-1}) and the observed vortex severity in the sump was indicated in parenthesis. A summary of each figure is provided below.

Figure 15 - W.S. EL 286 ft - Without Suppressors

> Angular velocity did not vary with Froude number ratio or Reynolds number, over the indicated range. Vortex severity increased with both Froude number ratio and Reynolds number.

Figure 16 - W.S. EL 286 ft - With Suppressors

Minimal change in angular velocity or vortex strength with Reynolds number or Froude number.

Figure 17 - W.S. EL 289 ft - Without Suppressors

Angular velocity tended to increase with Froude number ratio but not with Reynolds number. Severity increased with Froude number ratio, but essentially no variation with Reynolds number.

Figure 18 - W.S. EL 2899 ft - With Suppressors

Angular velocity showed some tendency to increase with Froude number ratio and Reynolds number. Little tendency for vortex severity to increase with Froude number ratio or with Reynolds number.

In general, vortex severity as measured by the vortimeter angular velocity and vortex type, tended to increase slightly with Froude number and with Reynolds number, as was expected from scaling considerations. With the suppressors in place, the worst type of vortex observed was Type 2. The shape of the vortex strength loci, as shown conceptionally in Figure 4, was evidently nearly horizontal with the suppressors in place, Figures 16 and 18. These plots indicate, therefore, that only Type 2 or lesser vortices would occur in the prototype.

None of the tests simulating fully or partially blocked doorways, gratings, or sump screens, produced flow patterns which had any stronger potential for vortices than was the case without blockage. Similarly, blockage of the upper 50% of the screens did not produce serious vortex activity. Complete blockage of the east doorway resulted in very low water levels in the sump room, along with very turbulent flow in the sump, thereby suppressing any vortex activity. Operating with either single line did not produce any more adverse flow patterns than occurred with both lines operating. Since the most critical flow patterns relative to vortex formation occurred with no blockage and both lines operating, most testing was directed towards characterizing vortex activity for those conditions.

CONCLUSIONS

The combination of gratings, screens, and vortex suppressors comprising Scheme 12 produced satisfactory results in the model with respect to vortex severity. Projection to prototype conditions based on the model vortex variation with Froude number ratio and Reynolds number, indicated that satisfactory flow conditions should be obtained in the prototype. More specifically, no vortices stronger than Type 3 seem possible under prototype operating conditions.

The associated intake loss coefficients were shown to increase with Reynolds number up to approximately $R = 10^6$, probably due to the effect of increasing swirl. The prototype intake loss coefficient will probably be 0.9 to 1.0 for line 2, and about 25% higher for line 1.

Single line operation did not appear to be more severe than with operation of both lines. Blockage of the west door, to simulate accumulated trash, was not critical to the flow conditions. Blockage of the east door also did not produce undesirable vortex activity, but did produce extremely turbulent flow patterns. Similarly, blockage of the upper 50% of the sump screen did not result in increased vortex activity.

REFERENCES

1. Young, Donald F., "Basic Principles and Concepts of Model Analysis," Experimental Mechanics, July 1971.

2. Daggett, L.L. and Keulegan, G.H., "Similitude in Free-Surface Vortex Formations," Journal of the Hydraulics Division, November 1974.

3. Reddy, Y.R. and Pickford, J., "Vortex Suppression in Stilling Pond Overflow," Journal of the Hydraulics Division, November 1974.

4. Hattersley, Ralph T., "Hydraulic Design of Pump Intakes," Journal of the Hydraulics Division, Proceedings of the American Society of Civil Engineers, March 1965.

5. Lee, Hsiao-Lien, "Swirling Flow in Inlets," M.S. Thesis, Worcester Polytechnic Institute, October 1975.

APPENDIX A

TEST PROGRAM

THREE MILE ISLAND NUCLEAR PLANT

EMERGENCY CORE COOLING SYSTEM – MODEL SUMP STUDY

TEST PROGRAM

TEST NO.	DATE	W.S. ELEVATION	FLOW GPM Q_1	FLOW GPM Q_2	DIRECTION EAST	DIRECTION WEST	WATER TEMPERATURE °F	CONFIGURATION	SCHEME
08-01	8/27/76	286.0	6,000	6,000	X	X	67.0	Trash racks at doors and platform	1
08-02	8/31/76	286.0	6,000	6,000	X	X	67.0	Trash racks at doors	2
08-03	8/31 [illegible]	286.0	5,000	5,000	X	X	67.0	Trash racks at doors	2
08-04	8/3[illegible]	286.0	4,000	4,000	X	X	67.0	Trash racks at doors	2
08-05	9/01/76	286.0	3,000	3,000	X	X	67.0	Trash racks at doors	2
08-06	9/01/76	286.0	2,500	2,500	X	X	67.0	Trash racks at doors	2
09-01	9/02/76	286.0	0	2,500	X	X	67.0	Trash racks at doors	2
09-02	9/02/76	286.0	2,500	0	X	X	67.0	Trash racks at doors	2
09-03	9/02/76	286.0	3,000	0	X	X	67.0	Trash racks at doors	2
09-04	9/03/76	286.0	[illegible]	3,000	X	X	66.0	Trash racks at doors	2
09-05	9/03/76	286.0	[illegible]	4,000	X	X	65.0	Trash racks at doors	2
09-06	9/03/76	286.0	4,000	0	X	X	65.0	Trash racks at doors	2
09-07	9/07/76	286.0	5,000	0	X	X	63.0	Trash racks at doors	2
09-08	9/07/76	286.0	0	5,000	X	X	63.0	Trash racks at doors	2

THREE MILE ISLAND NUCLEAR PLANT

EMERGENCY CORE COOLING SYSTEM – MODEL SUMP STUDY

TEST PROGRAM

TEST NO.	DATE	W.S. ELEVATION	FLOW GPM Q_1	FLOW GPM Q_2	DIRECTION EAST	DIRECTION WEST	WATER TEMPERATURE °F	CONFIGURATION	SCHEME
09-09	9/07/76	286.0	0	6,000	X	X	63.0	Trash racks at doors	2
09-10	9/08/76	286.0	6,000	0	X	X	63.0	Trash racks at doors	2
09-11	9/22/76	286.0	6,000	0	X	X	63.0	ARL screen design Trash racks at doors	5
09-12	9/22/76	286.0	6,000	0		X	63.0	ARL screen design Trash racks at doors	5
09-13	9/22/76	286.0	6,000	0	X		63.0	ARL screen design Trash racks at doors	5
09-14	9/22/76	286.0	6,000	0	X	X	63.0	ARL screen design Trash racks at doors, Scheme 1	6
09-15	9/22/76	286.0	6,000	0		X	63.0	ARL screen design Trash racks at doors, Scheme 1	6
09-16	9/22/76	286.0	6,000	0	X		63.0	ARL screen design Trash racks at doors, Scheme 1	6
09-17	9/23/76	286.0	6,000	0	X	X	63.0	ARL screen design Trash racks at doors, Scheme 2	7
09-18	9/23/76	286.0	6,000	0		X	63.0	ARL screen design Trash racks at doors, Scheme 2	7
09-19	9/24/76	286.0	6,000	0	X		62.0	ARL screen design Trash racks at doors, Scheme 2	7
09-20	9/24/76	286.0	6,000	0	X	X	62.0	Burns & Roe screen design Trash racks at doors	8
09-21	9/24/76	286.0	0	6,000	X	X	62.0	Burns & Roe screen design Trash racks at doors	8
09-22	9/24/76	286.0	6,000	6,000	X	X	62.0	Burns & Roe screen design Trash racks at doors	3

THREE MILE ISLAND NUCLEAR PLANT

EMERGENCY CORE COOLING SYSTEM – MODEL SUMP STUDY

TEST PROGRAM

TEST NO.	DATE	W.S. ELEVATION	FLOW GPM Q_1	FLOW GPM Q_2	DIRECTION EAST	DIRECTION WEST	WATER TEMPERATURE °F	CONFIGURATION	SCHEME
12-01	12/28/76	286.0	6,000	6,000	X	X	60.0	Final design	12
12-02	12/29/76	286.0	6,000	6,000	X		60.0	Final design	12
01-01	1/03/77	286.0	6,000	0	X	X	60.0	Final design	12
01-02	1/03/77	286.0	0	6,000	X	X	60.0	Final design	12
01-03	1/03/77	286.0	2,500	2,500	X	X	5[illegible]	Final design	12
01-04	1/04/77	286.0	2,500	0	X	X	[illegible]	Final design	12
01-05	1/04/77	286.0	0	2,500	X	X	62.0	Final design	12
01-06	1/04/77	286.0	6,000	6,000	X	X	62.0	Final design, upper 50% of screen blocked	12
01-07	1/04/77	286.0	6,000	6,000	X	X	100.0	Final design	12
01-08	1/05/77	286.0	6,000	6,000	X	X	140.0	Final design	12
01-09	/06/77	286.0	6,000	6,000	X	X	170.5	Final design	12
01-10	1/06/77	286.0	9,000	9,000	X	X	172.0	Final design	12
01-11	1/06/77	289.0	9,000	9,000	X	X	165.0	Final design	12
01-12	1/06/77	289.0	6,000	6,000	X	X	166.0	Final design	12

THREE MILE ISLAND NUCLEAR PLANT

EMERGENCY CORE COOLING SYSTEM – MODEL SUMP STUDY

TEST PROGRAM

TEST NO.	DATE	W.S. ELEVATION	FLOW GPM Q_1	FLOW GPM Q_2	DIRECTION EAST	DIRECTION WEST	WATER TEMPERATURE °F	CONFIGURATION	SCHEME
01-13	1/20/77	286.0	6,000	6,000	X	X	70.0	Final design, no vortimeter	12
01-14	1/21/77	286.0	6,000	6,000	X	X	60.0	Final design, no vortimeter	12
02-001	2/02/77	286.0	6,000	6,000		X	60.0	Final design	12
02-002	2/02/77	289.0	6,000	6,000	X	X	60.0	Final design	12
02-003	2/02/77	286.0	6,000	6,000	X	X	59.5	Final design, grating out	12
02-004	2/09/77	286.0	6,000	6,000	X	X	50.0	Final design	12
02-005	2/09/77	286.0	6,000	6,000	X	X	60.0	Final design	12
02-006	2/09/77	286.0	6,000	6,000	X	X	62.0	Final design, grating out	12
02-007	2/09/77	286.0	6,000	6,000	X	X	65.0	Final design, grating out	12
02-008	2/09/77	286.0	6,000	6,000	X	X	70.0	Final design, grating out	12
02-009	2/09/77	286.0	6,000	6,000	X	X	70.0	Final design, grating out	12
02-010	2/09/77	286.0	6,000	6,000	X	X	80.0	Final design	12
02-011	2/09/77	286.0	6,000	6,000	X	X	90.0	Final design	12
02-012	2/09/77	286.0	6,000	6,000	X	X	100.0	Final design	12

THREE MILE ISLAND NUCLEAR PLANT

EMERGENCY CORE COOLING SYSTEM – MODEL SUMP STUDY

TEST PROGRAM

TEST NO.	DATE	W.S. ELEVATION	FLOW GPM Q_1	FLOW GPM Q_2	DIRECTION EAST	DIRECTION WEST	WATER TEMPERATURE °F	CONFIGURATION	SCHEME
02-013	2/09/77	286.0	6,000	6,000	X	X	110.0	Final design	12
02-014	2/09/77	286.0	6,000	6,000	X	X	120.0	Final design	12
02-015	2/09/77	286.0	6,000	6,000	X	X	130.0	Final design	12
02-016	2/09/77	286.0	6,000	6,000	X	X	140.0	Final design	12
02-017	2/09/77	286.0	6,000	6,000	X	X	150.0	Final design	12
02-018	2/09/77	289.5	10,400	10,400	X	X	152.0	Final design	12
02-019	2/09/77	289.25	10,400	10,400	X	X	155.0	Final design, no grating	12
02-020	2/09/77	289.0	9,000	9,000	X	X	155.0	Final design, no grating	12
02-021	2/09/77	286.0	6,000	6,000	X	X	159.0	Final design, no grating	12
02-022	2/14/77	286.0	9,000	9,000	X	X	60.0	Final design, with grating	12
02-023	2/14/77	289.0	10,400	10,400	X	X	60.0	Final design, with grating	12
02-024	2/14/77	289.0	9,000	9,000	X	X	60.0	Final design, with grating	12
02-025	2/14/77	289.0	9,000	9,000	X	X	60.0	Final design, no grating	12
02-026	2/14/77	289.0	10,400	10,400	X	X	60.0	Final design, no grating	12

THREE MILE ISLAND NUCLEAR PLANT

EMERGENCY CORE COOLING SYSTEM – MODEL SUMP STUDY

TEST PROGRAM

TEST NO.	DATE	W.S. ELEVATION	FLOW GPM Q_1	FLOW GPM Q_2	DIRECTION EAST	DIRECTION WEST	WATER TEMPERATURE °F	CONFIGURATION	SCHEME
02-027	2/14/77	289.0	6,000	6,000	X	X	60.0	Final design, no grating	12
02-028	2/14/77	286.0	9,000	9,000	X	X	60.0	Final design, no grating	12

PHOTOGRAPHS

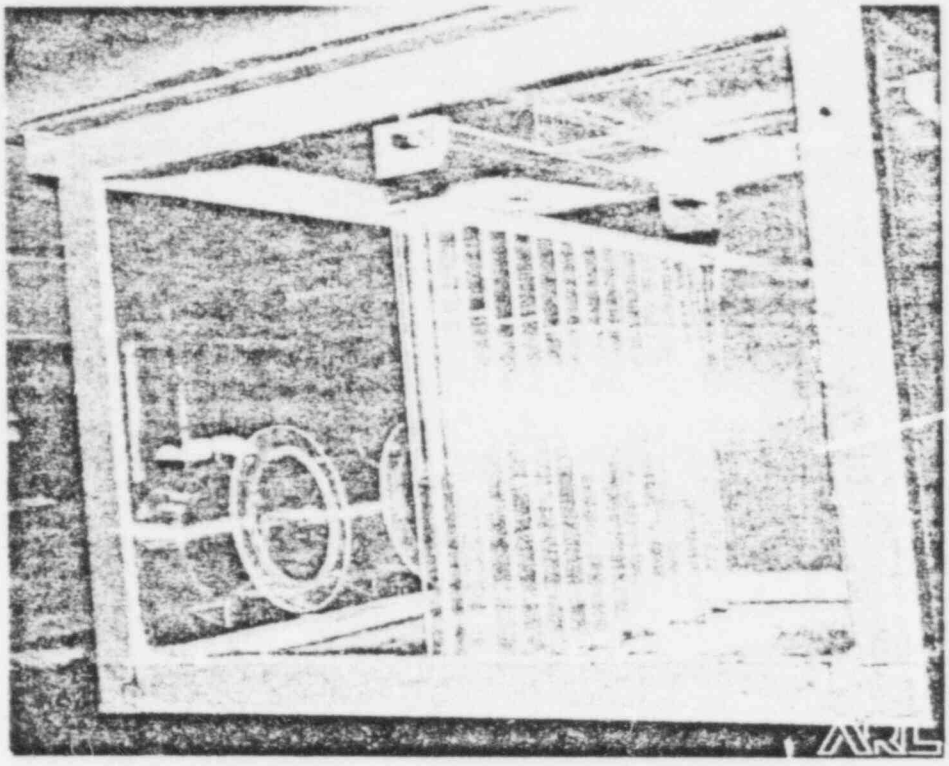

Photograph 1 Reactor Building Sump – Model

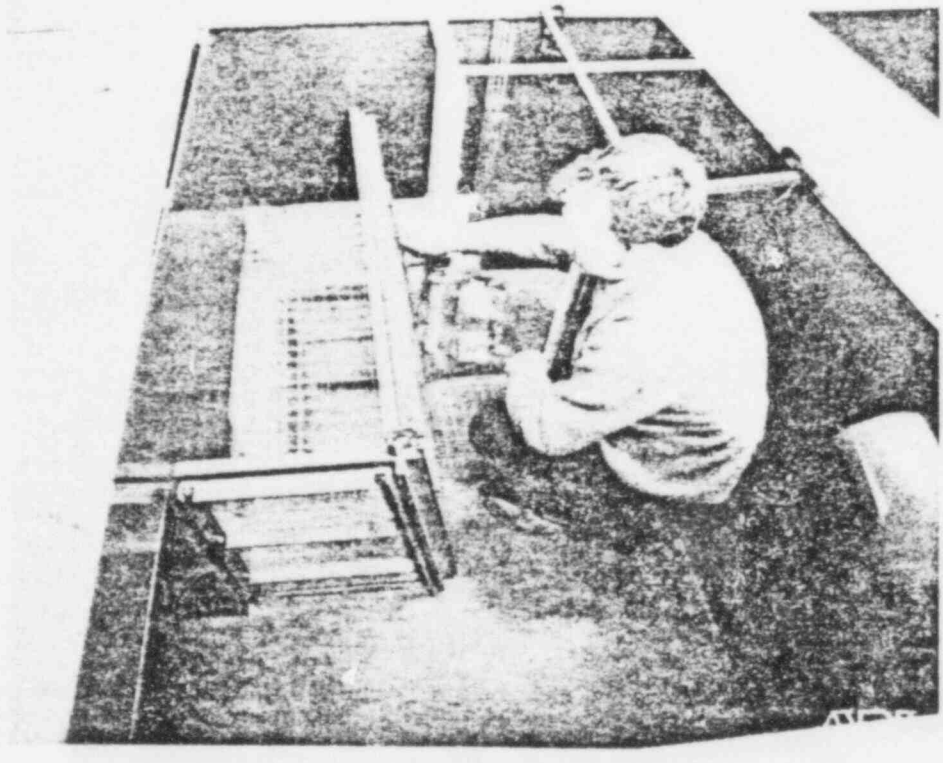

Photograph 2 Reactor Building Sump Room

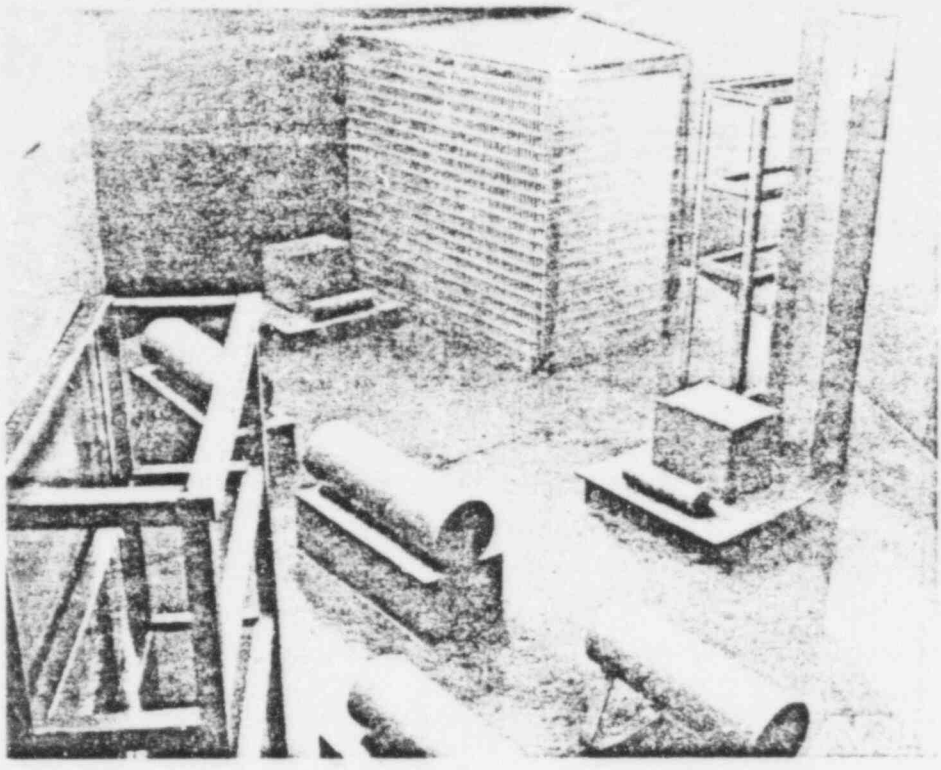

Photograph 3 East Sump Room Doorway

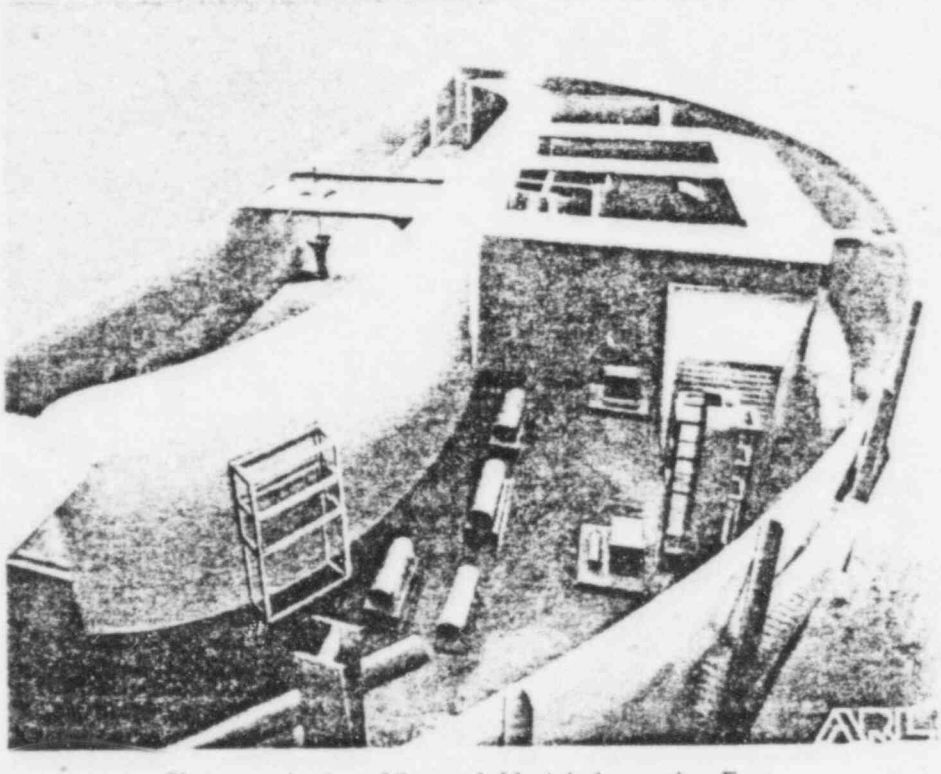

Photograph 4 View of Model from the East

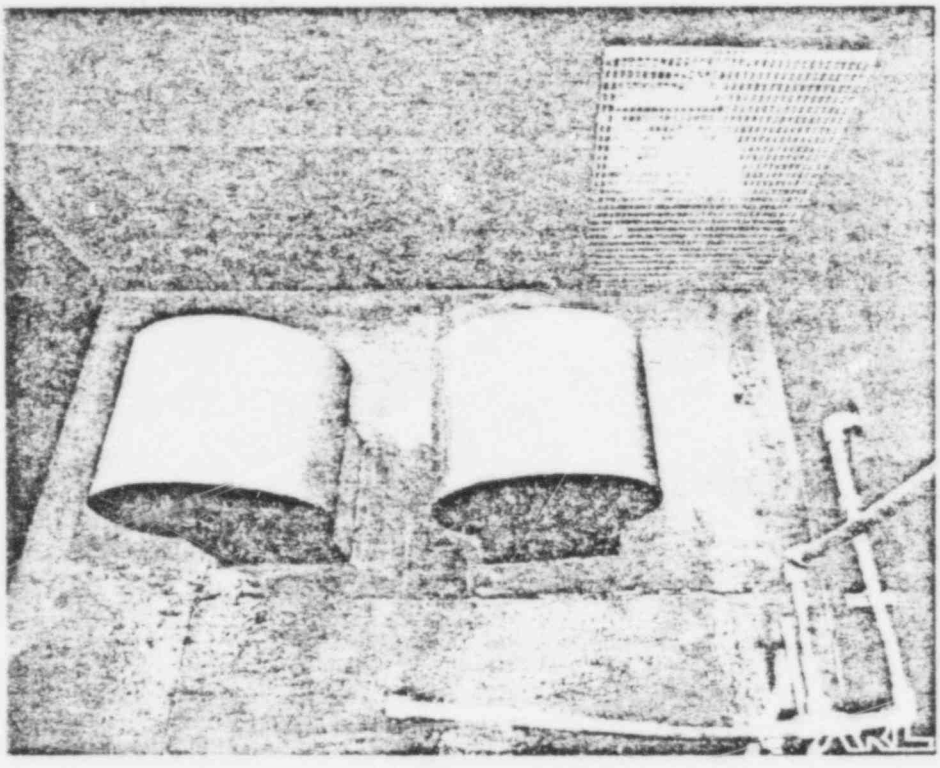

Photograph 5 West Sump Room Doorway

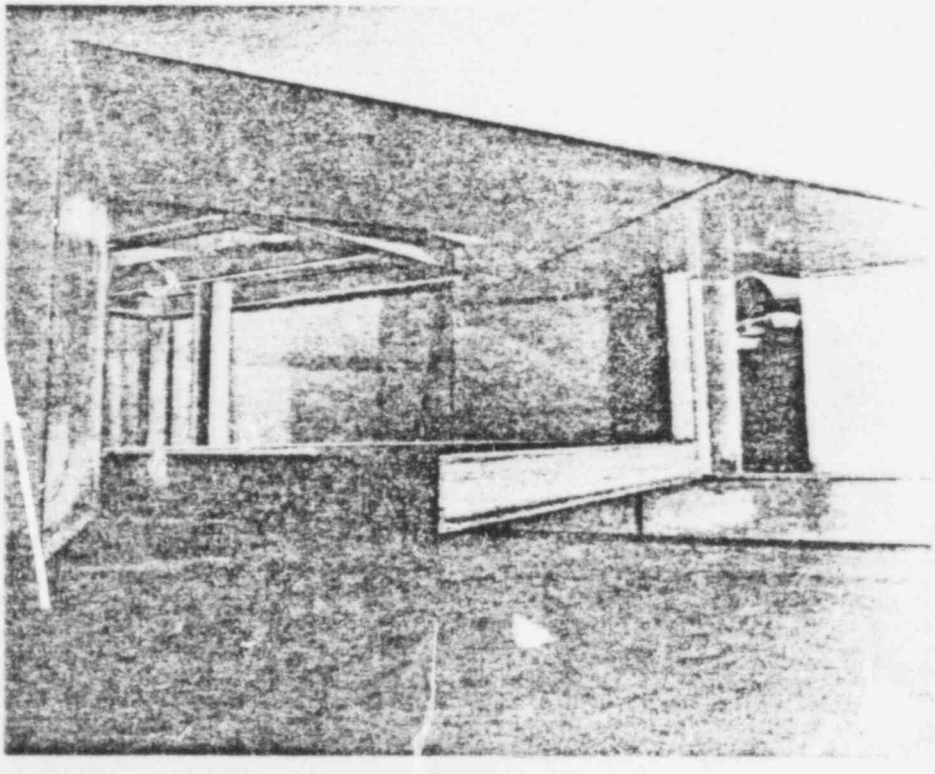

Photograph 6 View from Electrical Conduit Trench Towards West Doorway

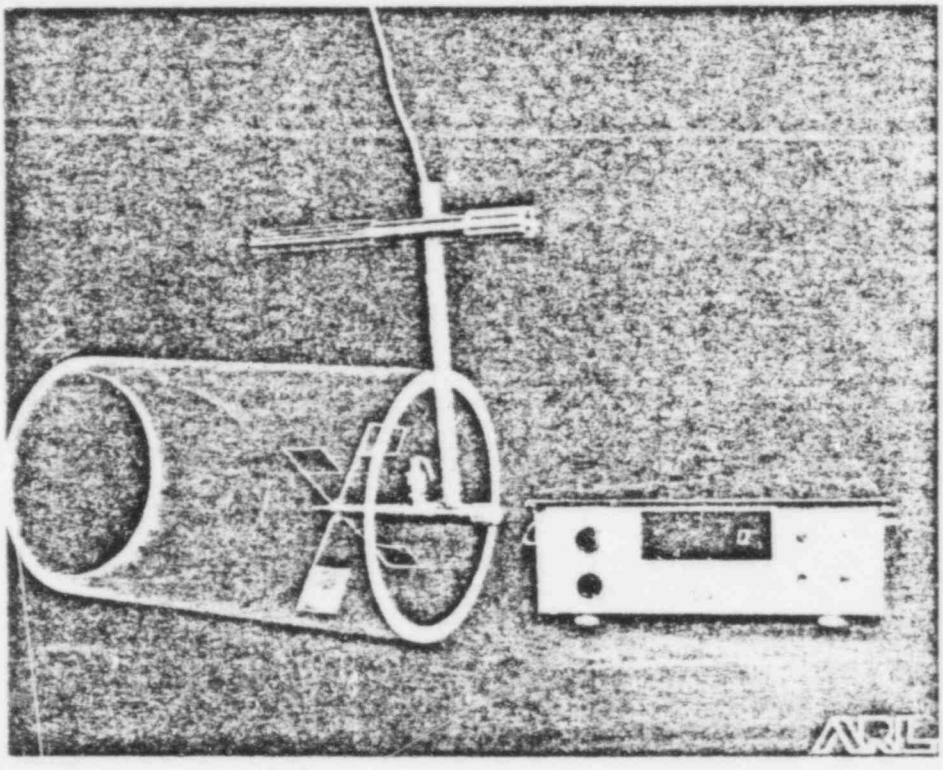

Photograph 7 Vortimeter

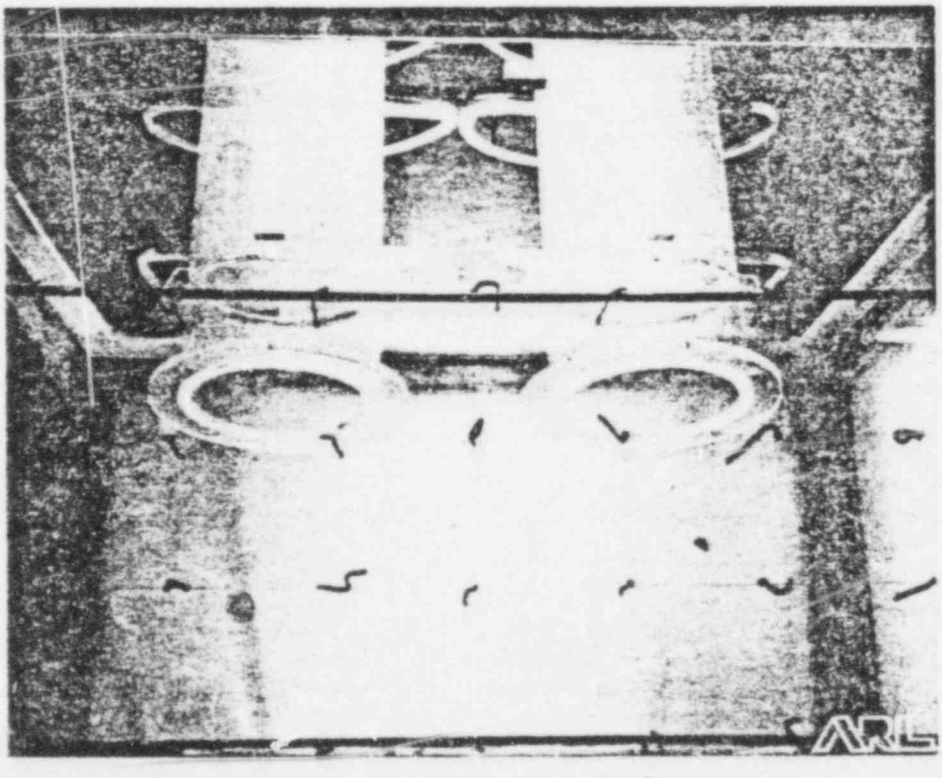

Photograph 8 Intake Lines with Piezometers

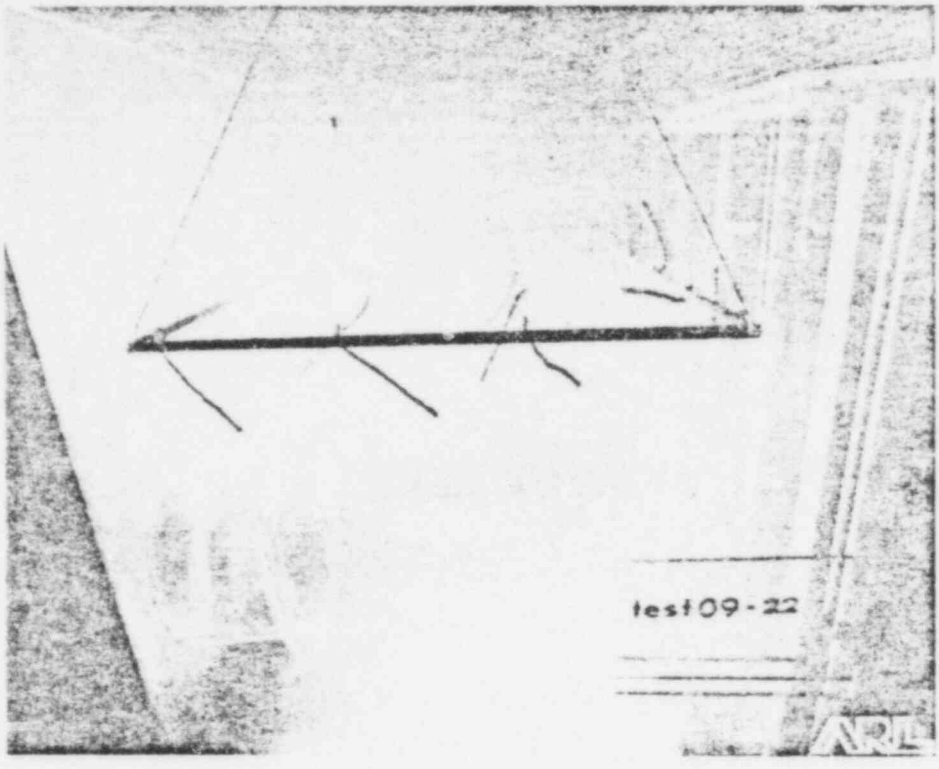

Photograph 9 Yarn Grid Showing Flow with Both Lines Operating

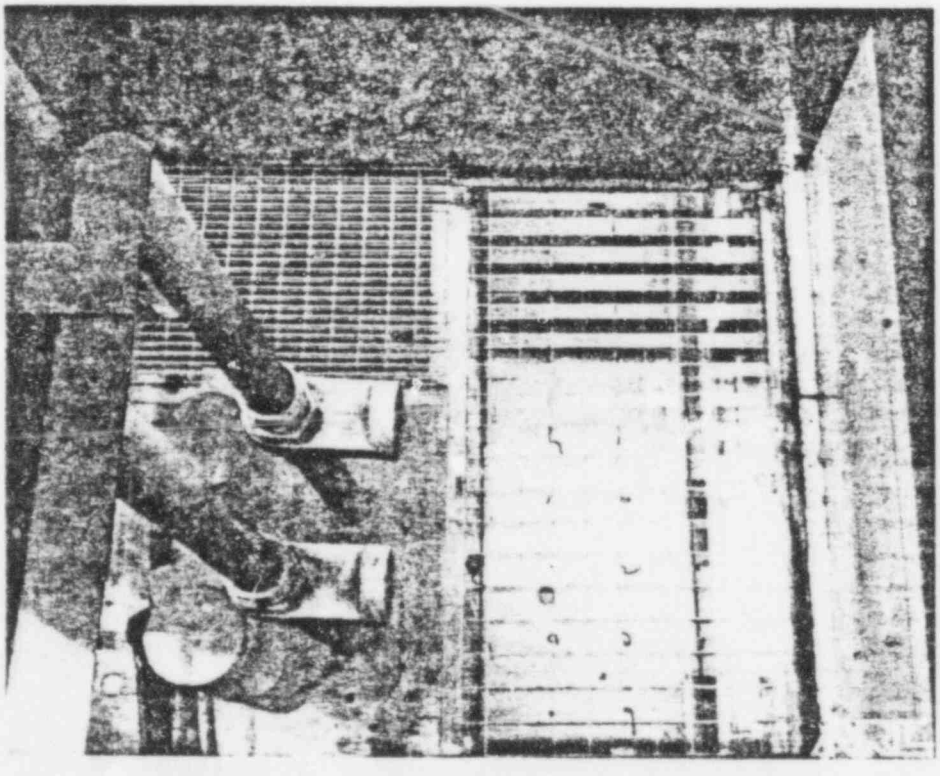

Photograph 10 Vortex Suppressor – Lower Level

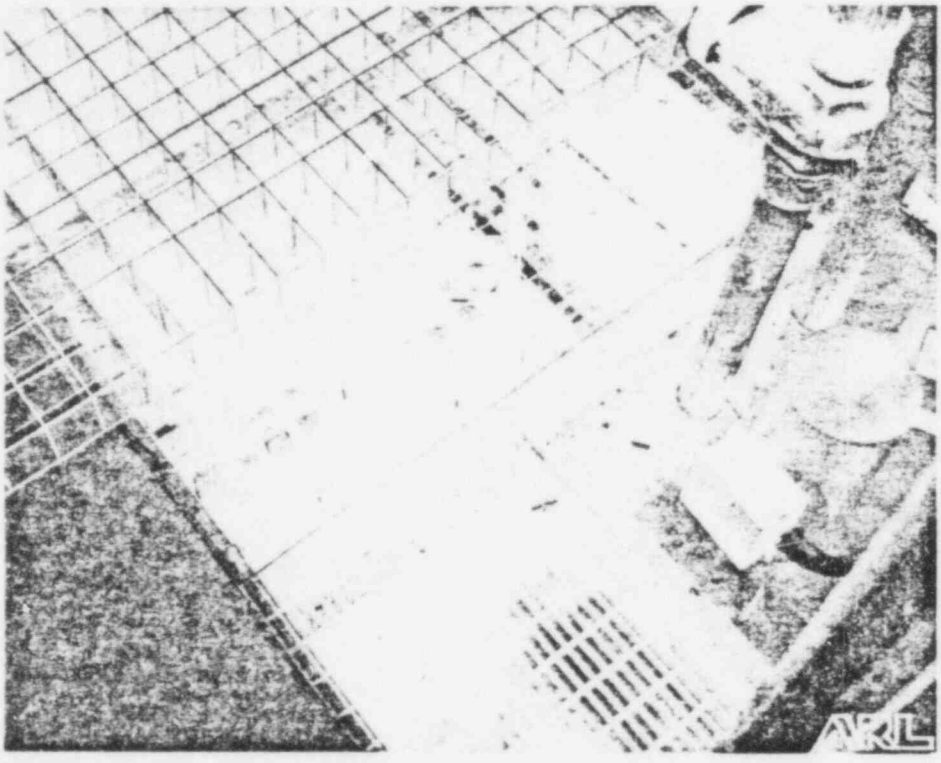

Photograph 11 Vortex Suppressors – Upper and Lower Levels

FIGURES

FIGURE 1

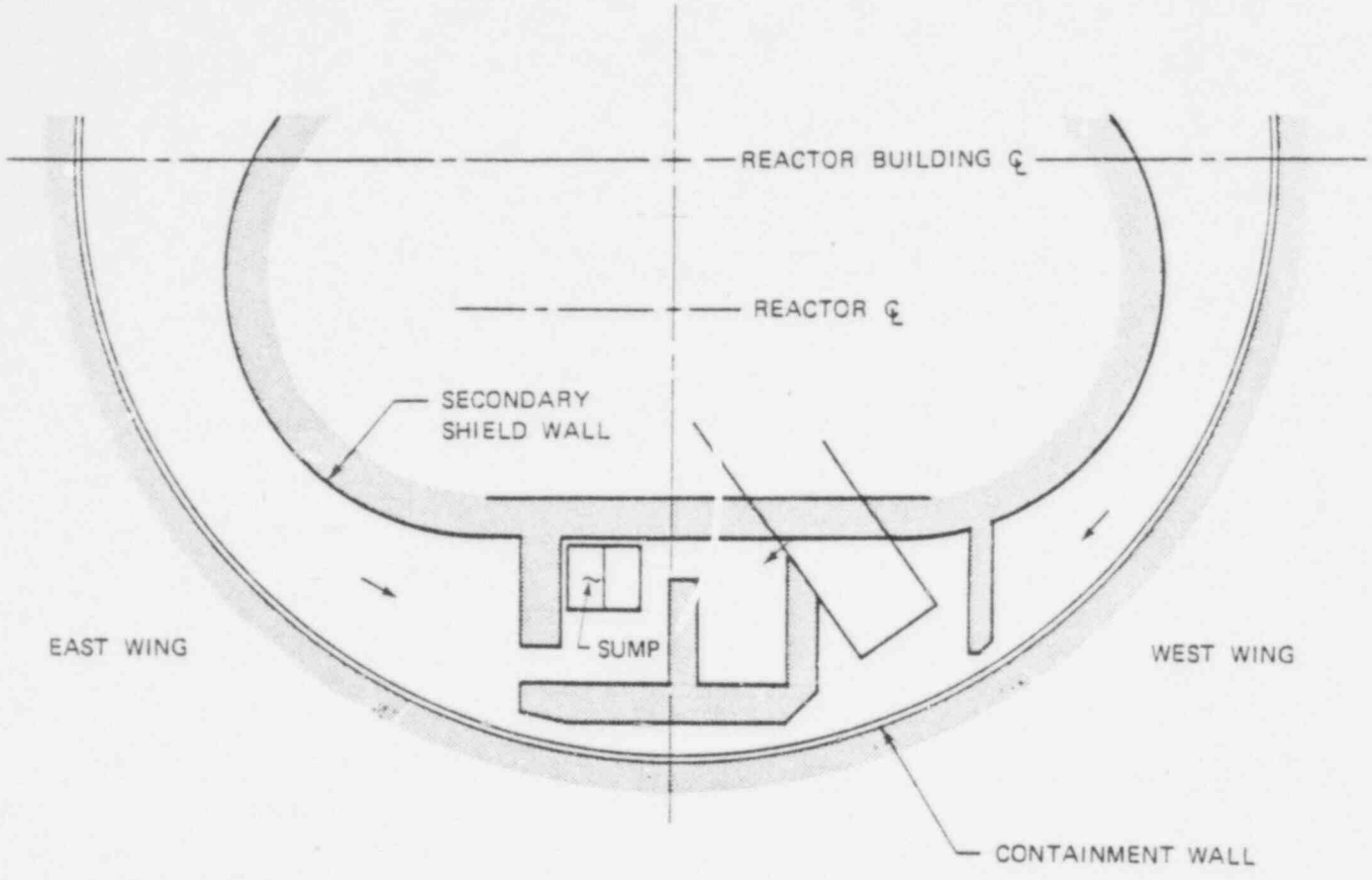

PLAN AT EL 282.5'

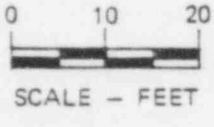

REACTOR BUILDING SUMP AREA

52-227

ARL

FIGURE 2

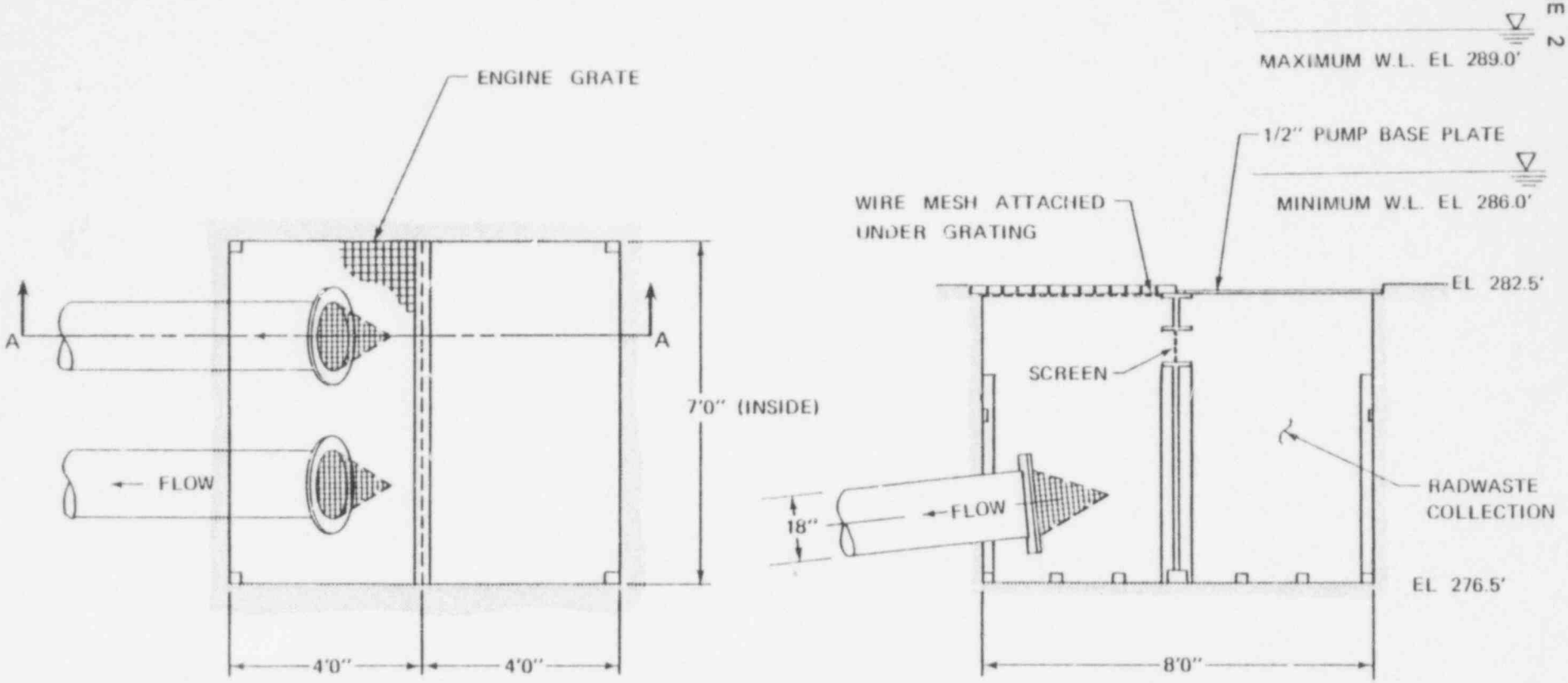

SUMP WITH ORIGINAL GRATE AND SCREENS

53-258

ARL

FIGURE 3

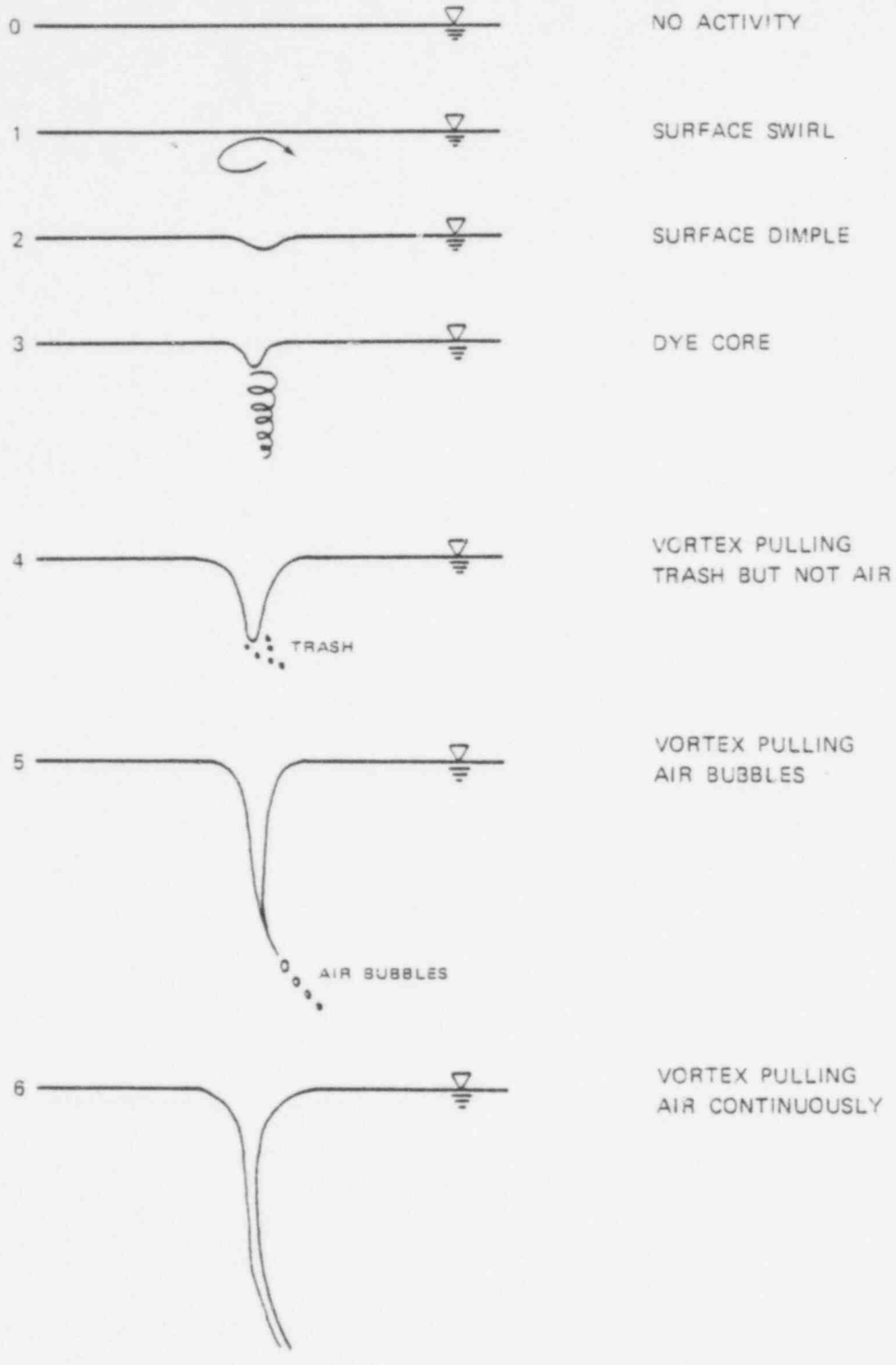

VORTEX STRENGTH SCALE
FOR INTAKE STUDY

53-269

ARL

FIGURE 4

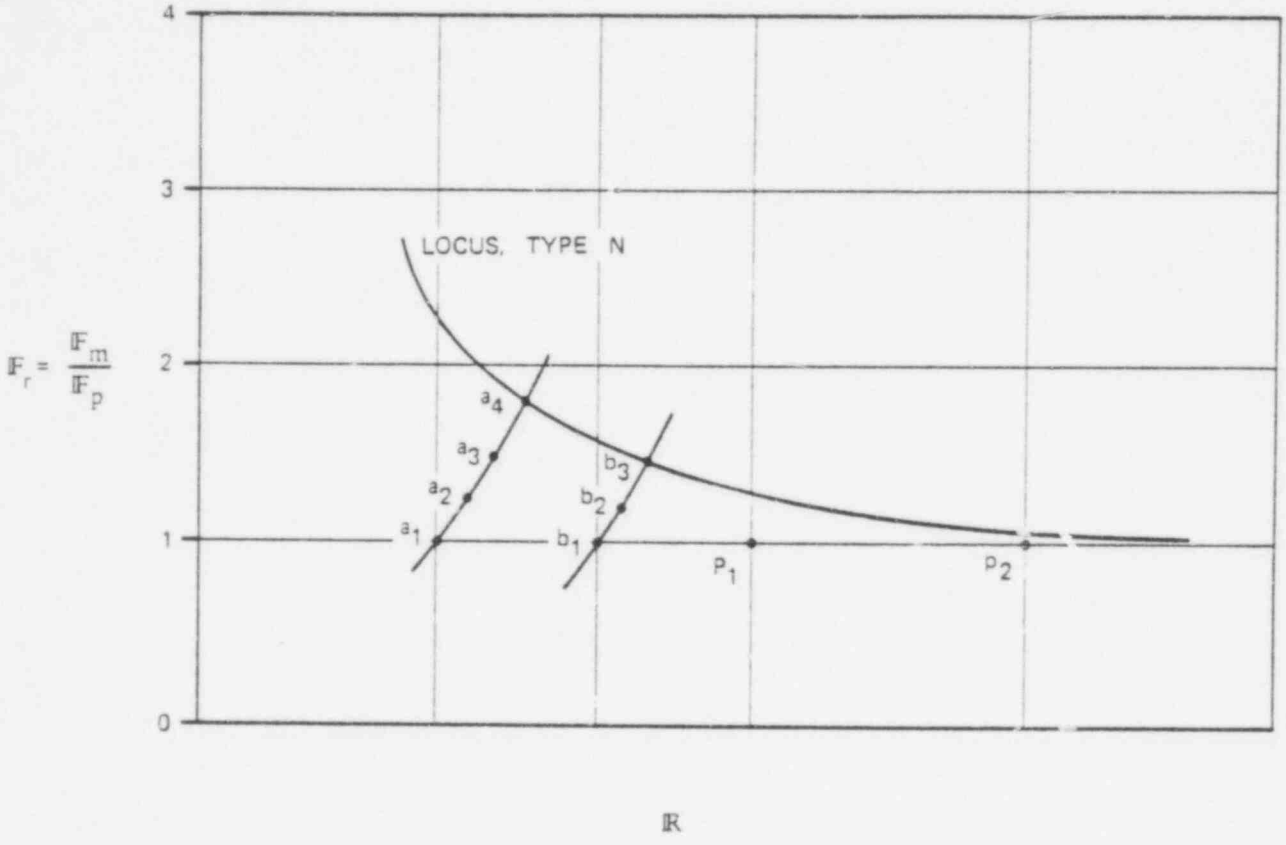

DEPENDENCE OF VORTEX SEVERITY ON
FROUDE AND REYNOLDS NUMBERS

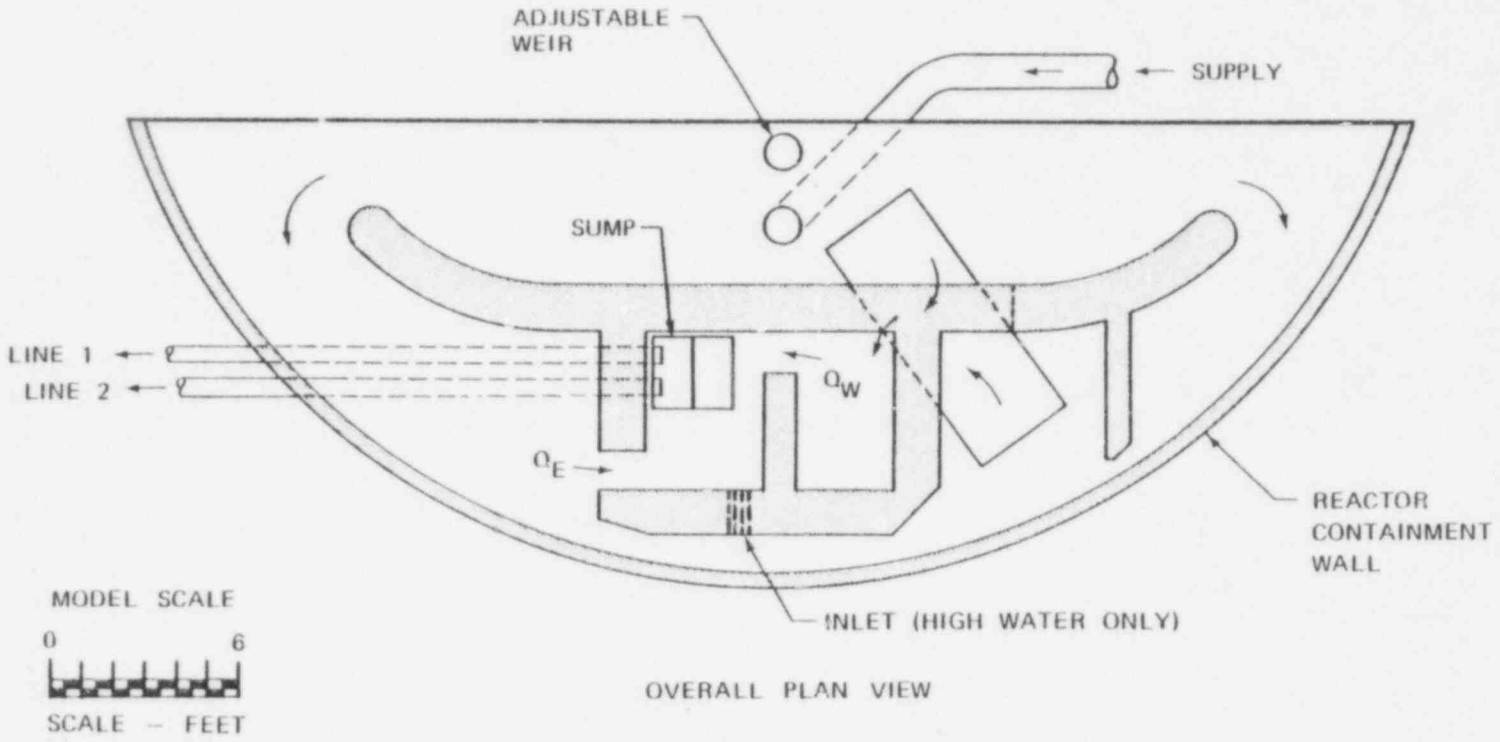

MODEL REACTOR BUILDING SUMP AREA

FIGURE 5

ARL

52-241

FIGURE 6

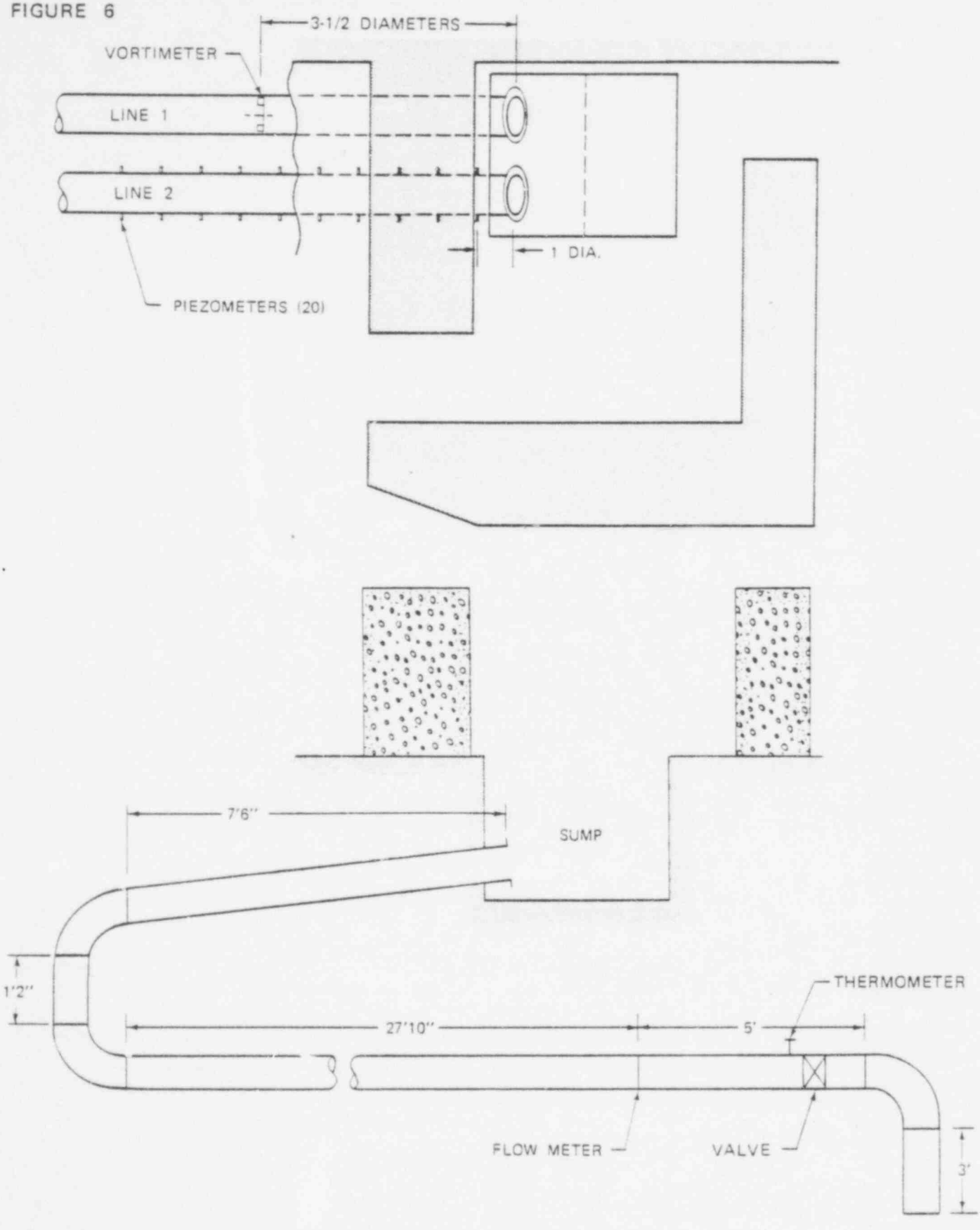

VORTIMETER AND PIEZOMETER INSTALLATION

ARL

FIGURE 7

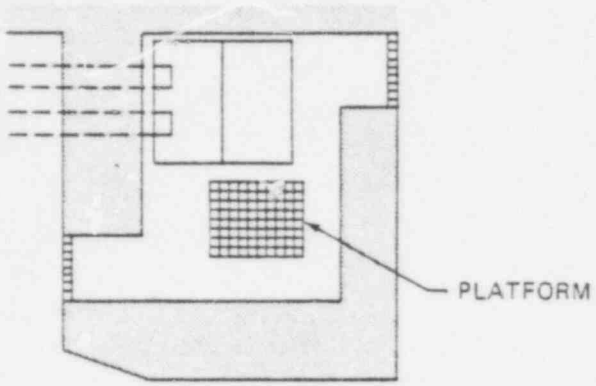

SCHEME 1

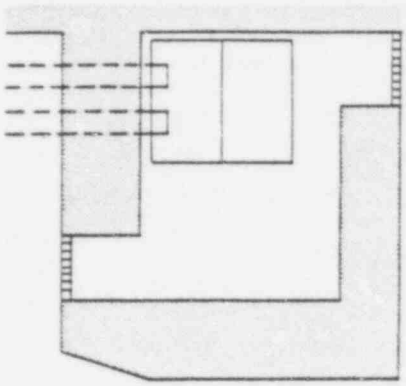

SCHEME 2

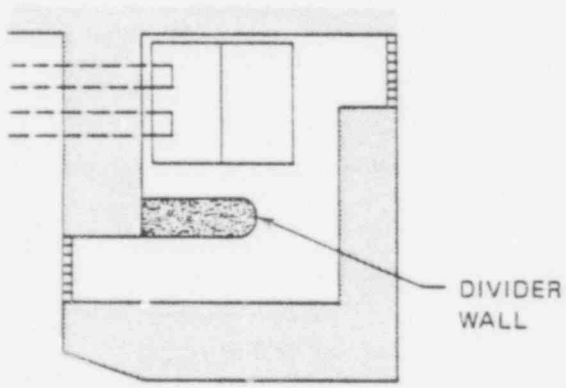

SCHEME 3

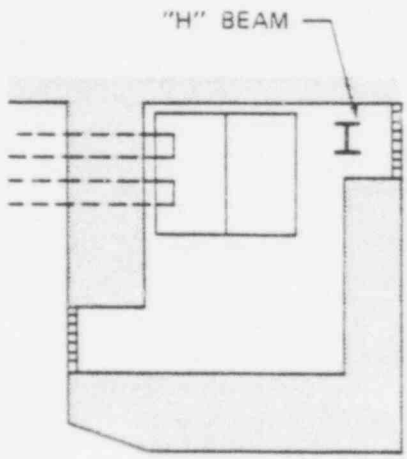

SCHEME 4

VORTEX SUPPRESSION SCHEMES INVESTIGATED
PHASE I

ARL

FIGURE 8

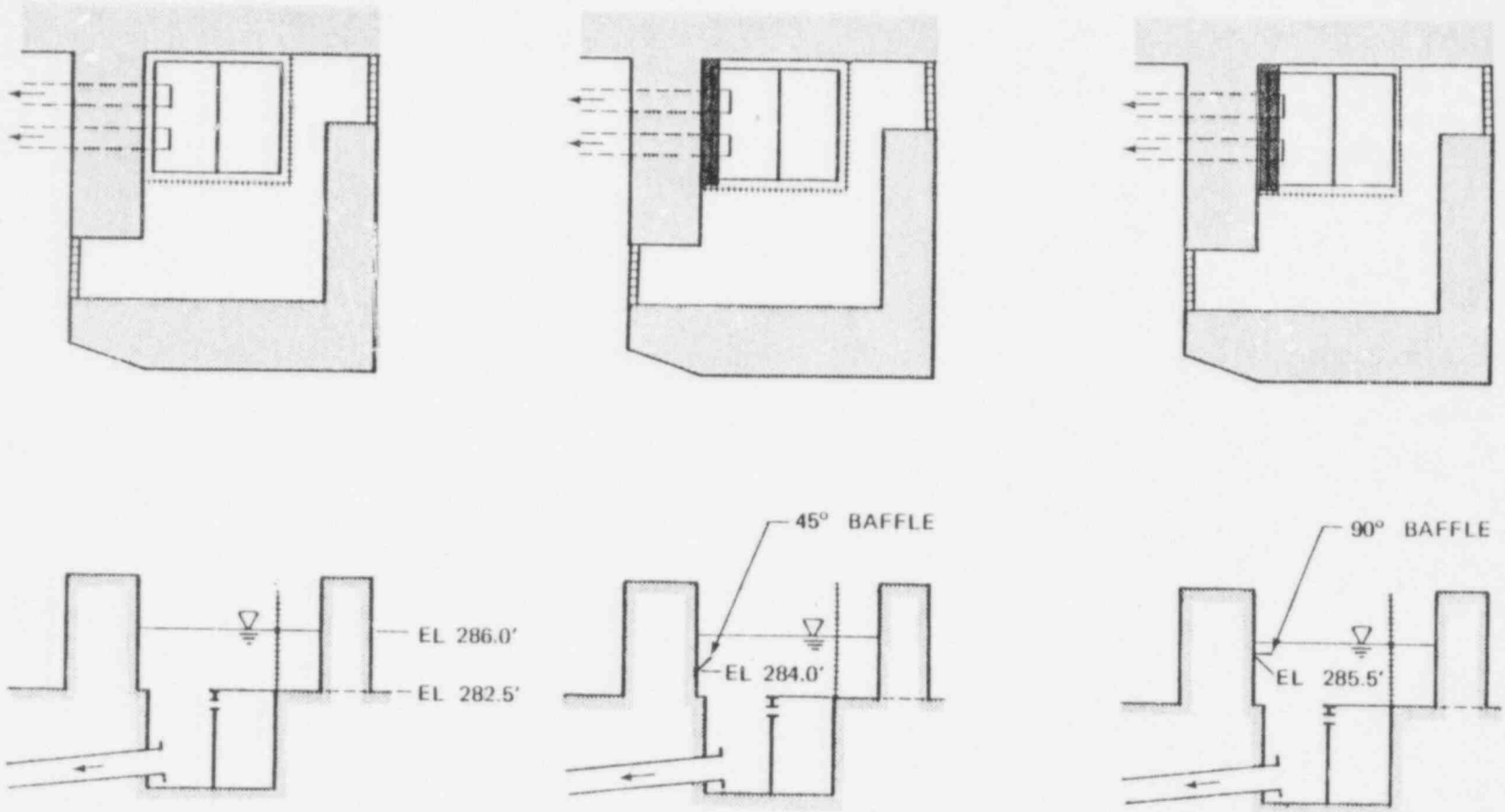

SCHEME 5

SCHEME 6

SCHEME 7

VORTEX SUPPRESSION SCHEMES INVESTIGATED
PHASE I

ARL

58-264

FIGURE 9

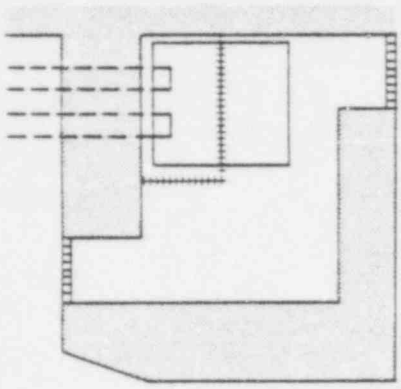

SCHEME 8

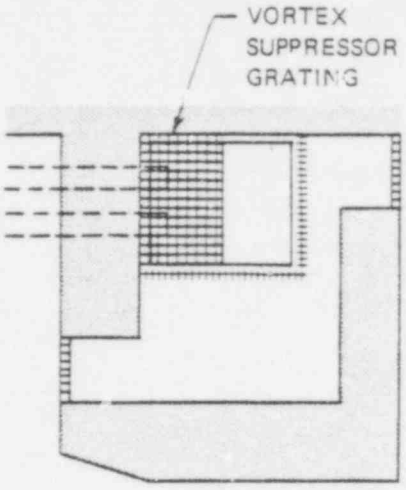

SCHEME 9

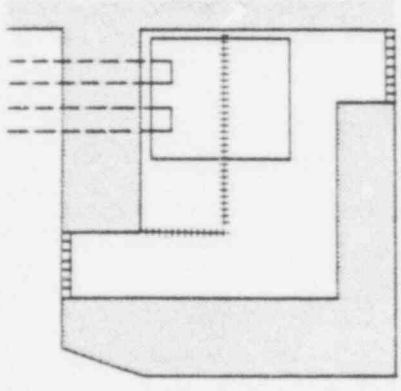

SCHEME 10

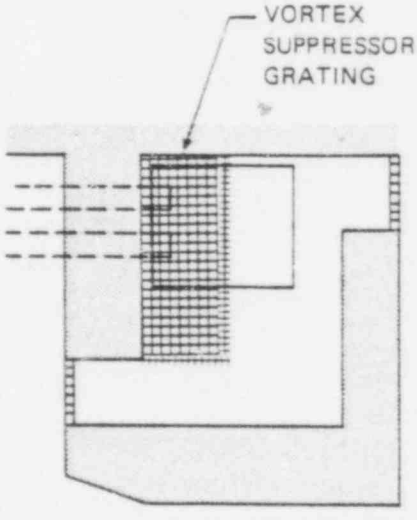

SCHEME 11

VORTEX SUPPRESSION SCHEMES INVESTIGATED
PHASE I

ARL

FIGURE 10

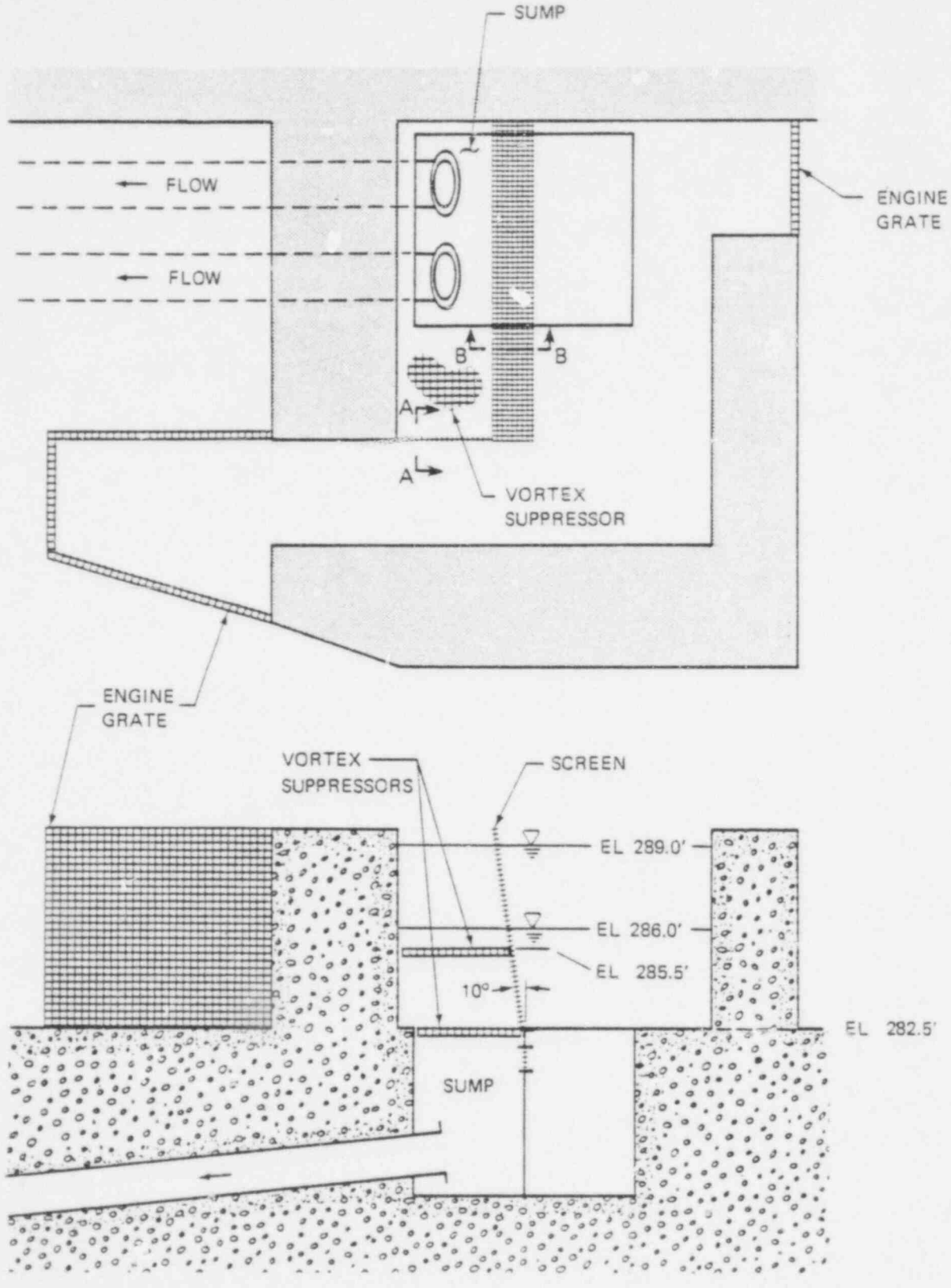

SCHEME 12 – PROPOSED FINAL DESIGN

FIGURE 11

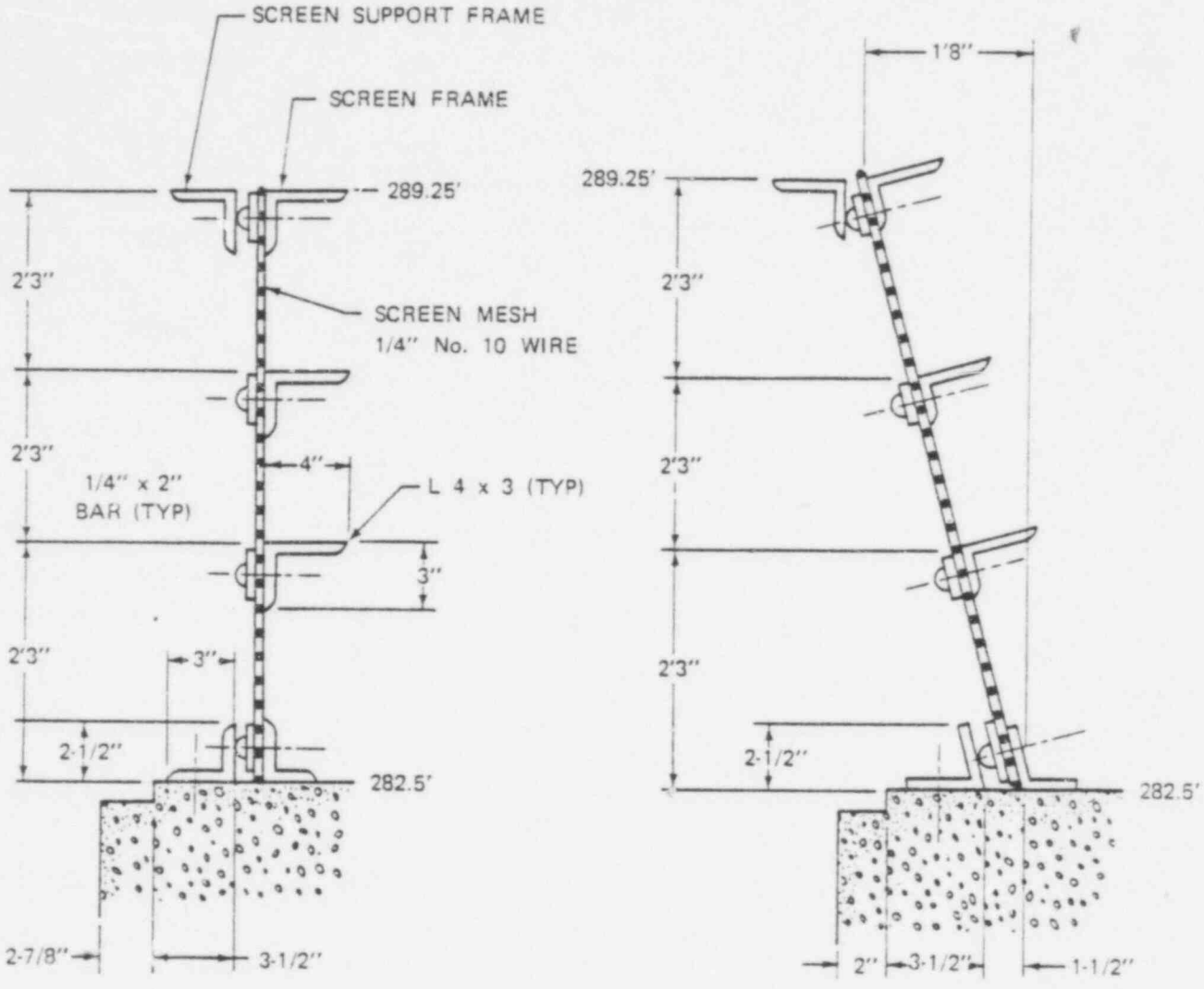

SECTION A-A

SECTION B-B

SUMP SCREEN DETAIL

52-247

ARL

FIGURE 12

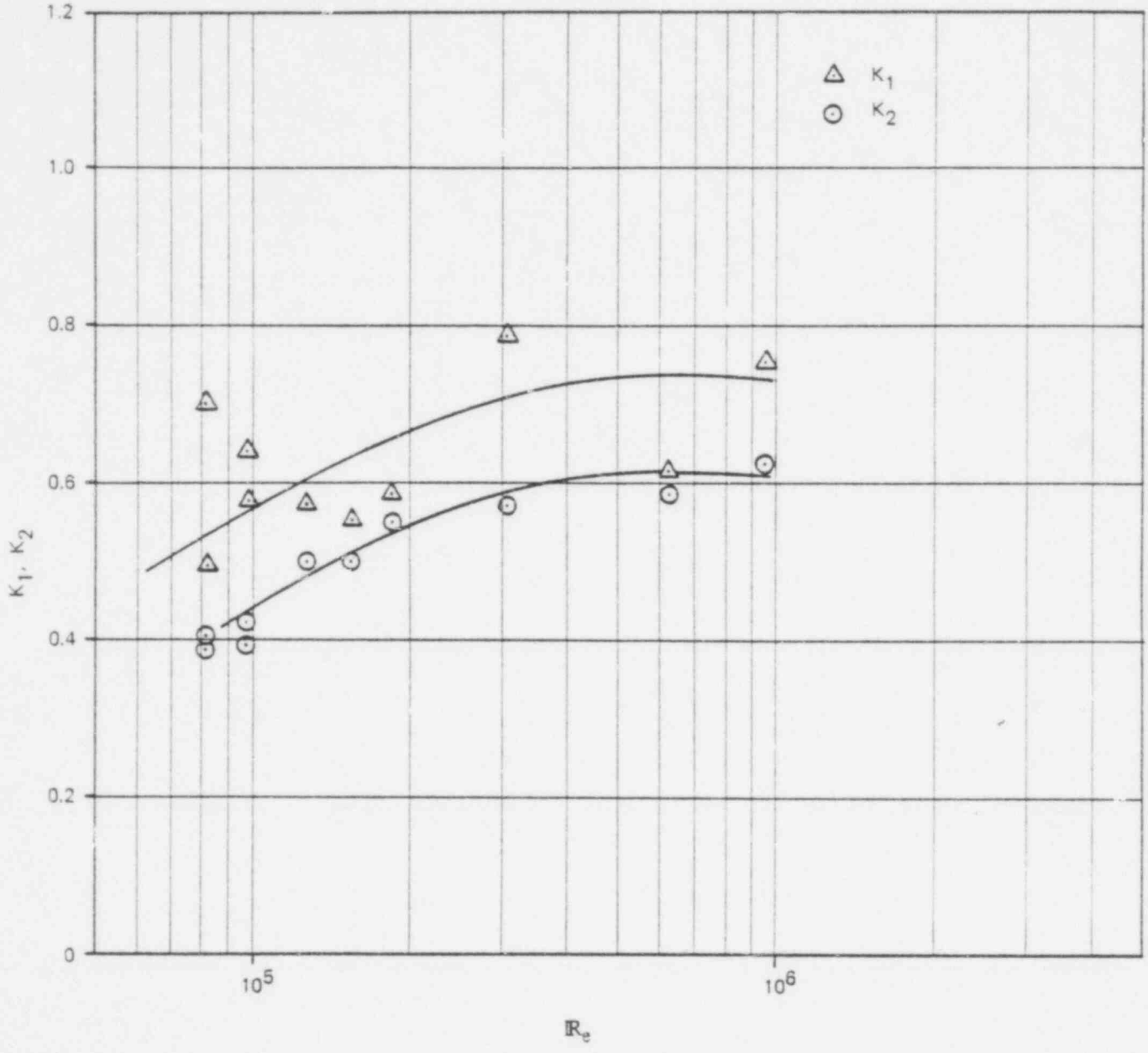

COMPARISON OF LOSS COEFFICIENTS'
VARIATION WITH REYNOLDS NUMBER
(SCHEME 2)

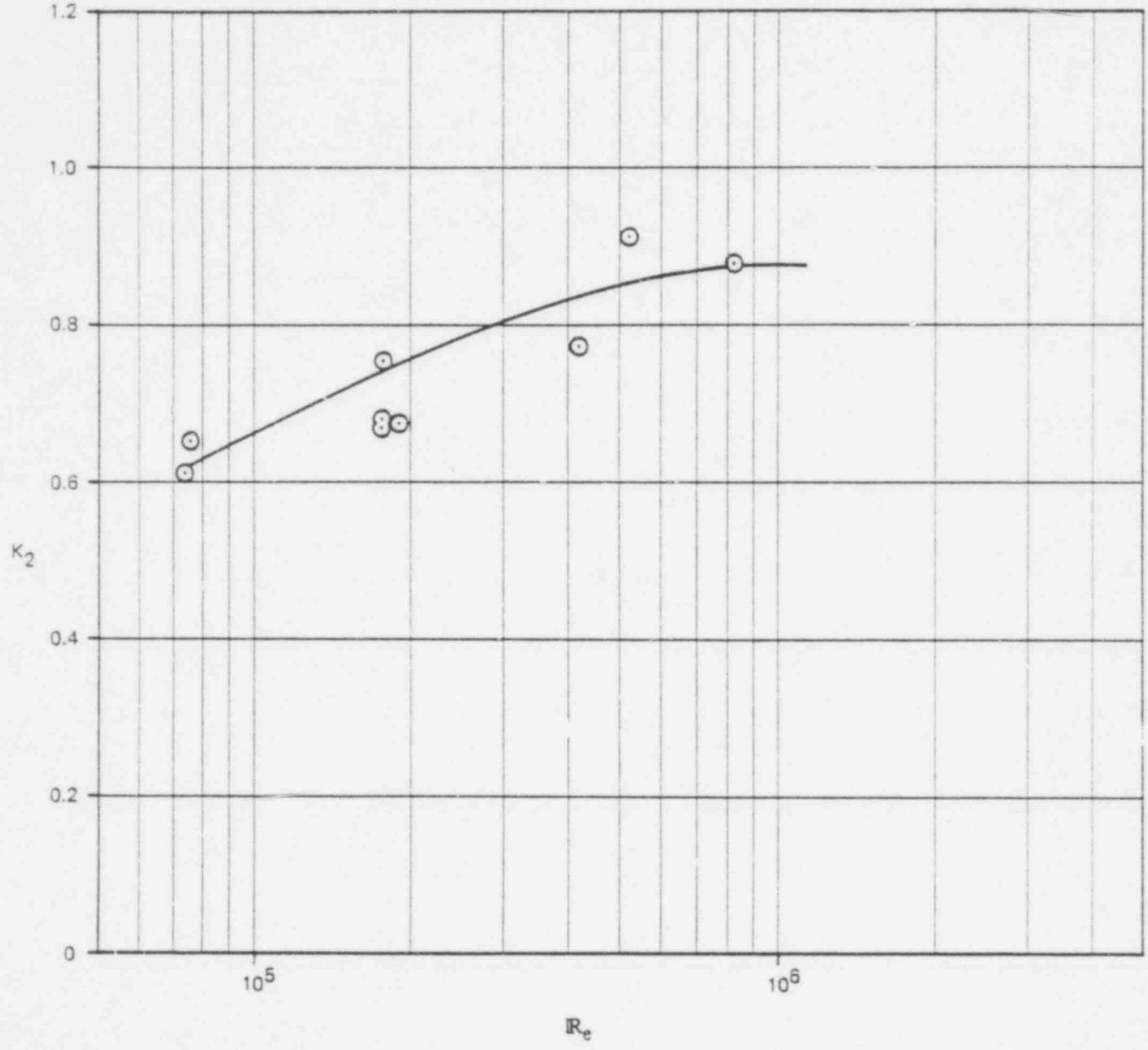

VARIATION OF LOSS COEFFICIENT WITH
REYNOLDS NUMBER, FINAL DESIGN
(SCHEME 12)

FIGURE 14

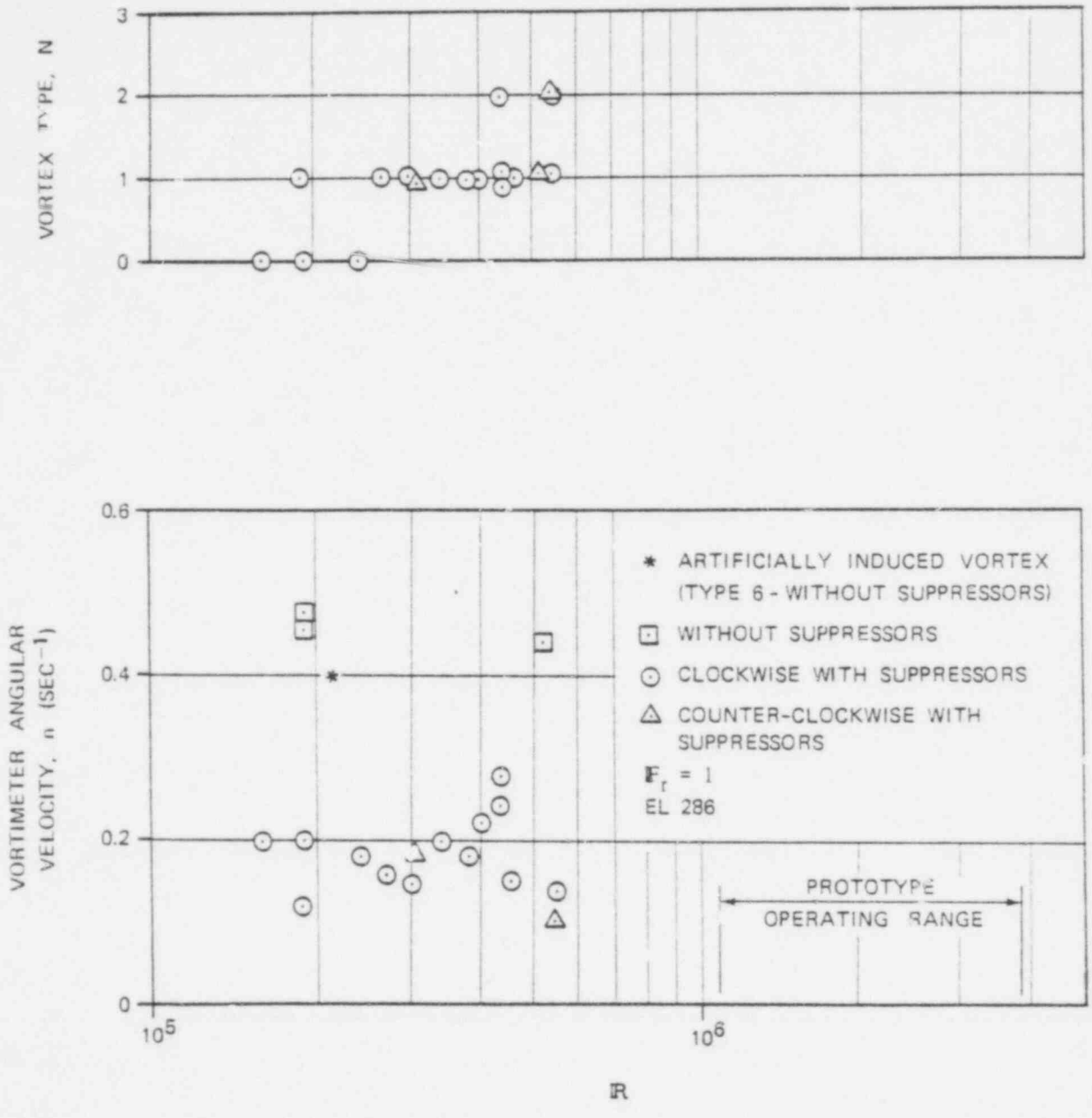

VORTIMETER ANGULAR VELOCITY AND
VORTEX TYPE VERSUS REYNOLDS NUMBER
SCHEME 12

52-750 ARL

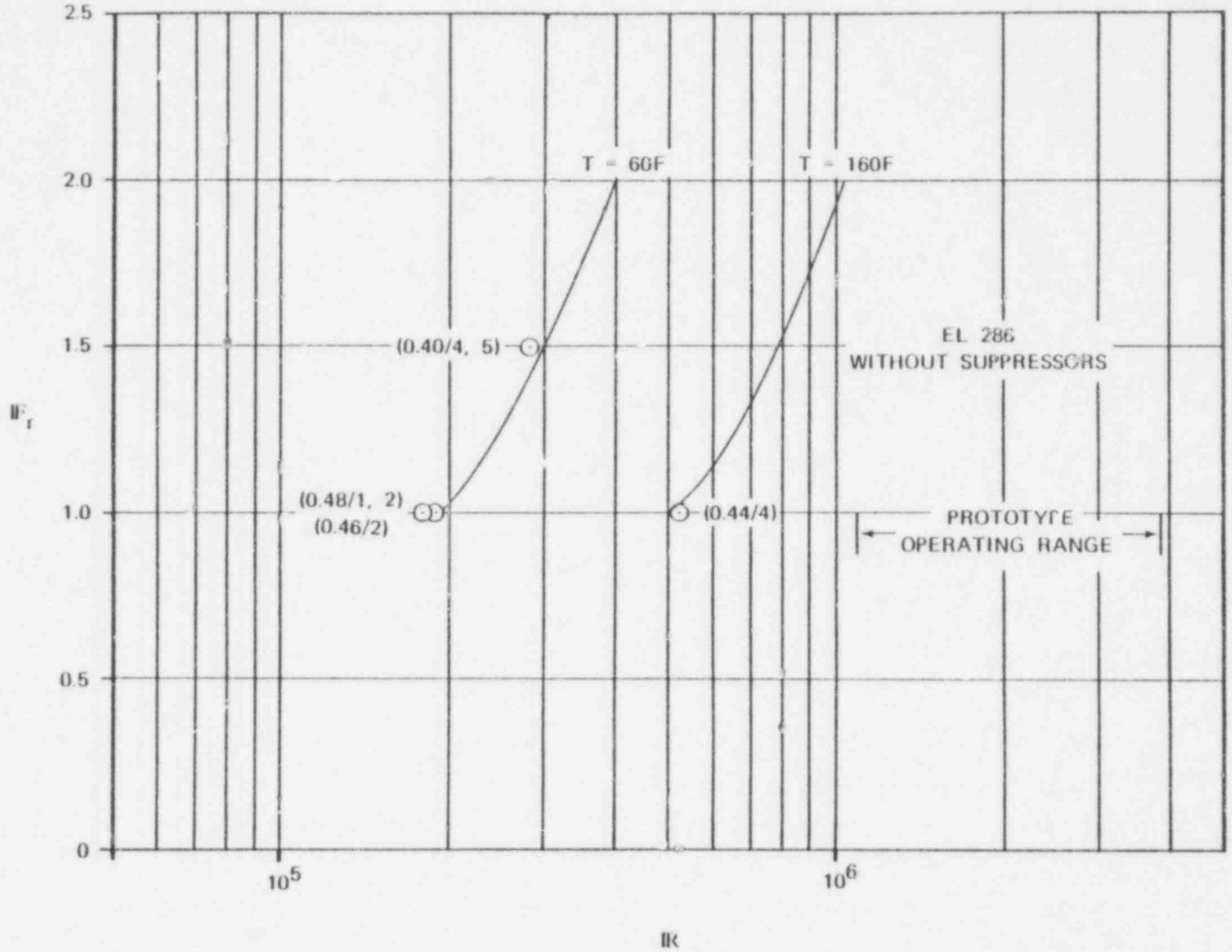

VORTIMETER READING AND VORTEX TYPE
VERSUS REYNOLDS AND FROUDE NUMBERS
SCHEME 12

FIGURE 15

ARL

FIGURE 16

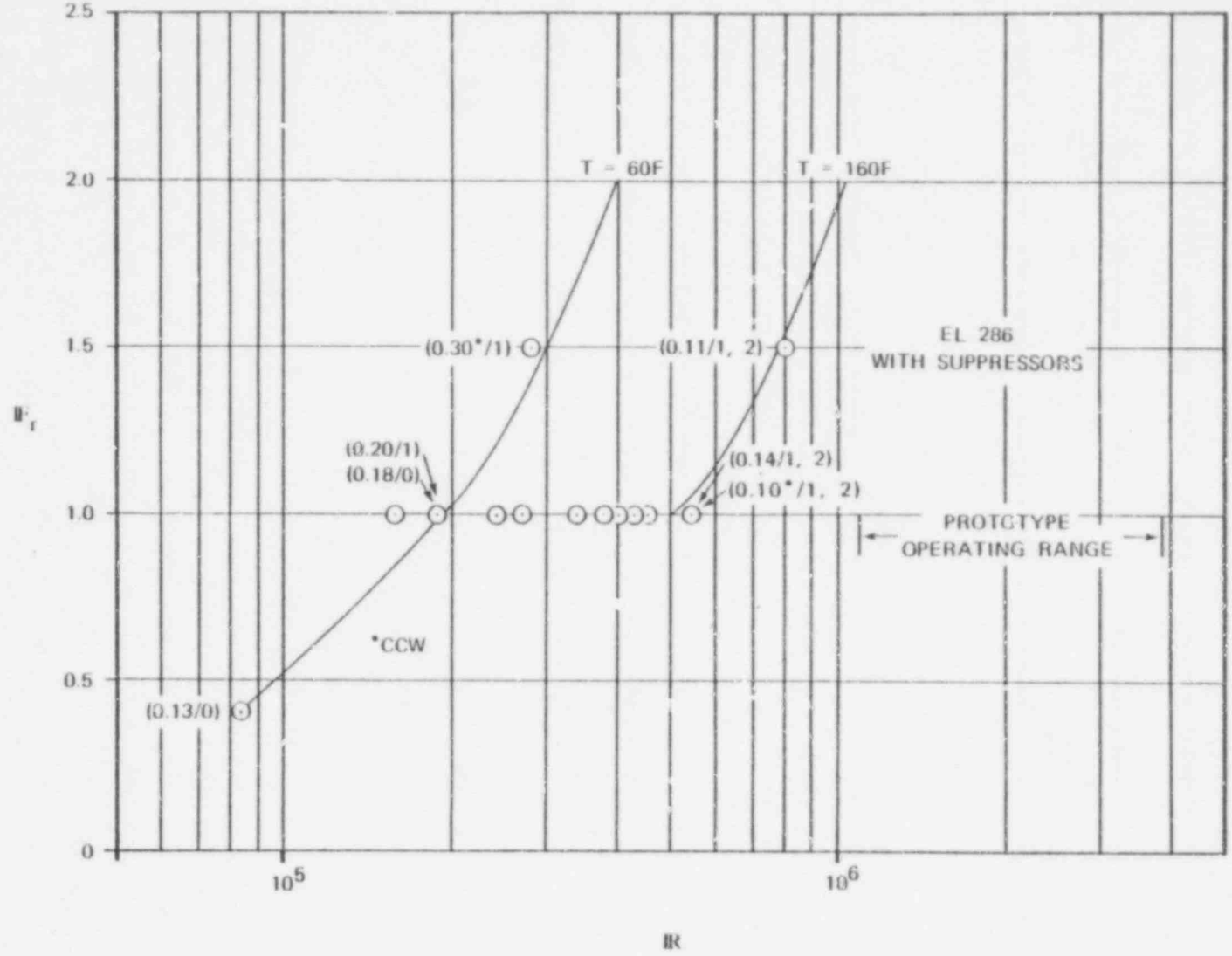

VORTIMETER READING AND VORTEX TYPE
VERSUS REYNOLDS AND FROUDE NUMBERS
SCHEME 12

ARL

FIGURE 17

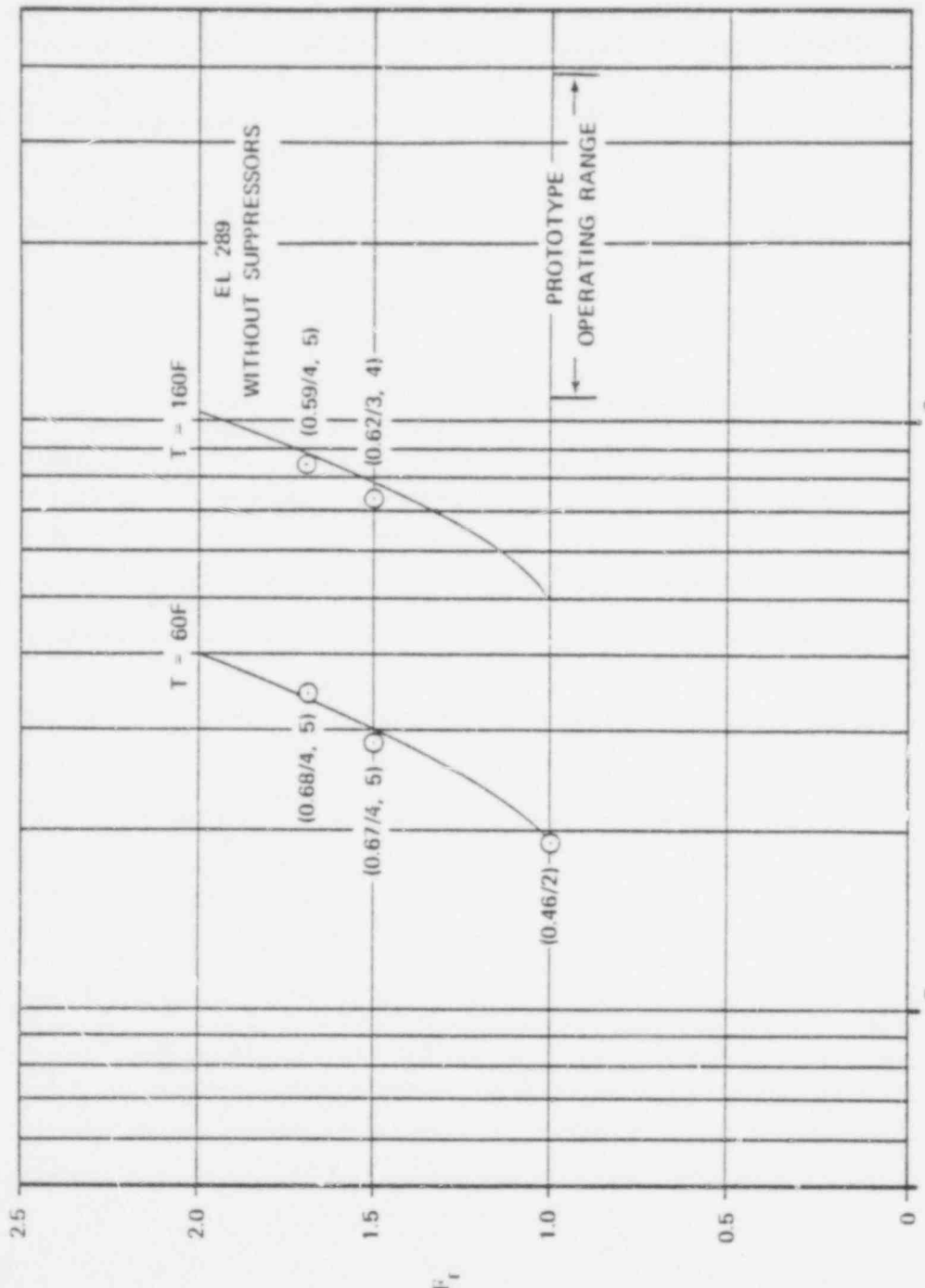

VORTIMETER READING AND VORTEX TYPE
VERSUS REYNOLDS AND FROUDE NUMBERS
SCHEME 12

52-253

FIGURE 18

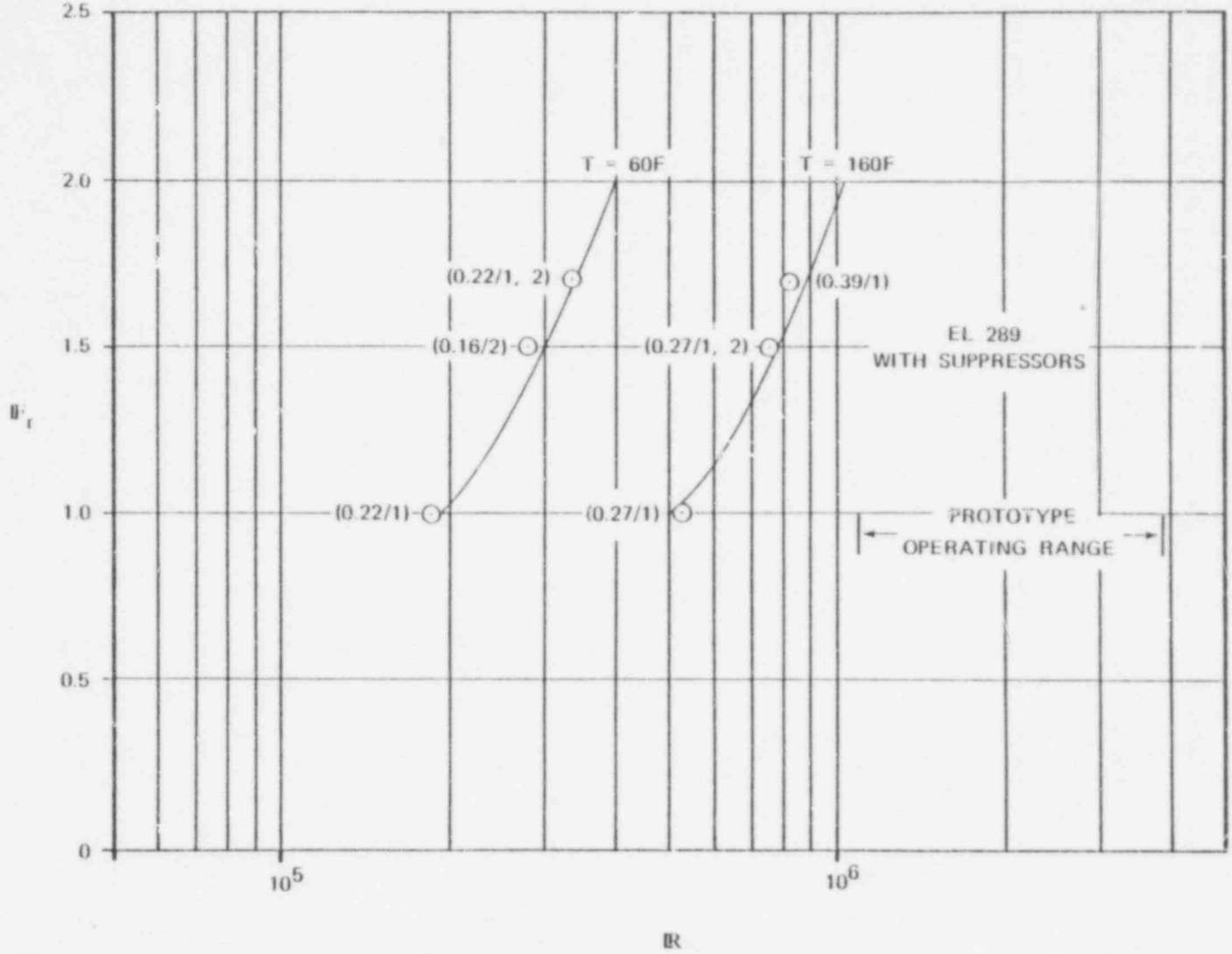

VORTIMETER READING AND VORTEX TYPE
VERSUS REYNOLDS AND FROUDE NUMBERS
SCHEME 12

ARL

52-214